Provisional Harvest Risk Assessment for the Southern Hudson Bay Polar Bear Subpopulation

Report to the Southern Hudson Bay Polar Bear Subpopulation Advisory Committee

07 June 2019

Prepared by: Eric Regehr* (University of Washington) and the Southern Hudson Bay Polar Bear Technical Working Group (Markus Dyck, Gregor Gilbert, Samuel Iverson, David Lee, Nicholas Lunn, Joseph Northrup, Alan Penn, Marie-Claude Richer, and Guillaume Szor)

*Corresponding author: Eric V. Regehr, E-mail: eregehr@uw.edu

Please cite as: Regehr, E., M. Dyck, G. Gilbert, S. Iverson, D. Lee, N. Lunn, J. Northrup, A. Penn, M.-C. Richer and G. Szor. 2019. Provisional Harvest Risk Assessment for the Southern Hudson Bay Polar Bear Subpopulation. Report to the Southern Hudson Bay Polar Bear Subpopulation Advisory Committee, 07 June 2019. Unpublished report. 75 pp.

Executive Summary

The Southern Hudson Bay Technical Working Group (TWG) was formed to provide advice to the Southern Hudson Bay Polar Bear Subpopulation Advisory Committee. The TWG has recently compiled the available scientific data for the Southern Hudson Bay (SH) subpopulation, summarized historical removal levels, worked with an outside expert to construct a demographic model, performed a harvest risk assessment, and documented these steps in the current report to the Advisory Committee. Although the assessment was based primarily on scientific information, Indigenous Knowledge was considered when interpreting and modeling the status of the SH subpopulation. The TWG is not a decision-making body. Rather, it sought to draw upon the expertise of its membership to develop and provide advice to the responsible decision-making bodies for the SH subpopulation.

This report presents a quantitative harvest risk assessment for the SH polar bear subpopulation. The final results are a series of potential harvest strategies that can inform prospective management actions in conjunction with other sources of information and considerations. The assessment uses a custom demographic model that was developed to evaluate responses to different environmental conditions and management interventions. Population processes are represented by a discrete version of the theta-logistic equation, which is widely used in ecology. The model includes a single age class and is applied to female bears only. This approach is consistent with the limited demographic information available for the SH subpopulation. The model includes a nonlinear relationship between population density and population growth resulting in demographic patterns that are generally within the bounds of those documented for polar bears and similar species. The model can incorporate the potential effects of habitat change through both density-dependent mechanisms (i.e., changing environmental carrying capacity [K]) and density-independent mechanisms (i.e., changing maximum intrinsic growth rate [r_{max}]).

We estimated parameters of the theta-logistic equation using a Bayesian Monte Carlo approach to population reconstruction. This process used estimates of abundance and population growth rate from capture-recapture studies in the 1980s and 2000s (Obbard et al.

2007), estimates of abundance from aerial surveys in the 2010s (Obbard et al. 2015, 2018), and harvest data from Nunavut, Québec, and Ontario. It also allowed incorporation of prior information from other case studies of polar bears. Population reconstruction demonstrated that the demographic model can reproduce plausible trends for the SH subpopulation in recent decades.

The available data are not conclusive regarding the current demographic status of the SH subpopulation. Statistical uncertainty and methodological differences between capture-recapture studies and aerial surveys preclude estimation of long-term trends in abundance. Several lines of evidence suggest that the subpopulation was, on average, capable of strong growth during the period 1984-2016 and thus could support a relatively high harvest. However, there is also evidence for a decline from 943 bears in 2012 (Obbard et al. 2015) to 780 bears in 2016 (Obbard et al. 2018) based on aerial surveys with consistent methodology. Sea ice has declined in the SH management area, although to a lesser extent than other polar bear management areas (Stern and Laidre 2016), and the SH subpopulation has experienced declines in nutritional condition (Obbard et al. 2016). In the adjacent Western Hudson Bay (WH) subpopulation, similar declines in condition were detected prior to obtaining evidence from capture-recapture studies for declines in reproduction, survival, and abundance (Lunn et al. 2016). Recent aerial surveys for the WH subpopulation suggest a decline in numbers during the period 2011-2016 based on multiple lines of evidence, although the difference in abundance estimates was not statistically significant (Stapleton et al. 2014; Dyck et al. 2017).

We accounted for uncertainty in the current and future status of the SH subpopulation by developing three biological scenarios representing a plausible range of conditions, from optimistic to pessimistic, based on the available scientific data and documented Indigenous Knowledge. The scenarios were developed using different approaches to population reconstruction and different assumptions about the future effects of habitat loss. Scenario 1 reflected the optimistic hypothesis that the future will be similar to the past 30 years, with only gradual declines in K proportional to projected declines in the number of ice-covered days per year in the SH management area. Scenario 2 reflected the middle-of-the-road hypothesis that the future will be similar to the past decade, during which there is some evidence of

demographic declines, and that both K and r_{max} will decline gradually in the future. Scenario 3 consisted of two pessimistic representations of the SH subpopulation. Scenario 3a included a strong density-independent decline in r_{max} followed by gradual declines in both K and r_{max}. Scenario 3b reflected a subpopulation that was theoretically capable of strong growth but experienced rapid and nonlinear declines in K.

For each biological scenario, we used the demographic model to project simulated polar bear subpopulations forward in time while being subject to a wide range of female harvest rates. Projections were run for 35 years, which corresponds to approximately three polar bear generations and is a common timeframe for conservation assessments (Regehr et al. 2016). We evaluated the effects of harvest against three potential alternatives for subpopulation Management Objectives: (1) maintain a subpopulation size that achieves maximum sustainable yield, with respect to a potentially changing K; (2) maintain a relatively stable subpopulation size; and (3) maintain a subpopulation size above a minimum threshold, below which the function and viability of the subpopulation are likely to be compromised. Management Objective 3 is not intended as a measure of sustainability, but rather to indicate whether the subpopulation could become depleted to the extent that emergency management measures might be warranted. We present the probabilities of achieving the three management objectives for multiple harvest strategies, rather than only presenting results for a smaller number of harvest strategies that correspond to predetermined levels of risk tolerance (i.e., that correspond to specific probabilities of meeting the objectives).

We can compare results for the three biological scenarios by looking at harvest strategies with an 80% probability of meeting Management Objective 1 (i.e., maintaining a subpopulation size that achieves maximum sustainable yield). Management Objective 1 is well suited to balancing subpopulation protection with continued opportunities for use, and an 80% probability falls between the “low” and “medium” levels of risk tolerances that have been subjectively used for Management Objective 1 in other harvest assessments (Regehr et al. 2017a, 2018a). Furthermore, harvest strategies that meet these conditions were associated with low probabilities of violating Management Objective 3 or reducing future sustainable yield through overharvest. For Scenario 1, the corresponding harvest strategy had a present-day

harvest level of 21 female bears/year. This is similar to the mean observed harvest for the SH subpopulation of approximately 19 females/year for the period 1986-2016, which is logical given that Scenario 1 was based on the hypothesis that the future will be similar to the past. For Scenario 2, the starting harvest level was 10 female bears/year. Assuming that the proportion of females in the SH subpopulation is currently 0.50, this would correspond to a total (i.e., female and male) harvest rate of approximately 3.8% if harvest were implemented at a 2:1 male-to-female ratio. For reference, this is slightly below the 4.5% rate at a 2:1 male-to-female ratio that has been considered sustainable under favorable environmental conditions (Taylor et al. 1987). For Scenario 3a, the starting harvest level was 4 female bears/year. The probability of violating Management Objective 3 increased at a starting harvest level of 8 female bears/year, and the probability of extirpation increased at a starting harvest level of 18 female bears/year. Scenario 3a demonstrates the potential for overexploitation when a subpopulation's capacity for growth is compromised by severe density-independent limitation. In contrast, subpopulation outcomes for Scenario 3b were relatively insensitive to harvest. This is because the rapid and unidirectional decline in *K* guaranteed that abundance would decline as well, and natural mortality due to density effects could be largely replaced by harvest without accelerating subpopulation declines. Although Scenarios 3a and 3b are both oversimplifications of how sea-ice loss might impact the SH polar bear subpopulation, they demonstrate the importance of whether the effects of habitat change are primarily density independent or density dependent. Currently, the data are not available to differentiate between density-independent and density-dependent effects for SH bears, and this remains an area of research for polar bears in general.

Our approach of considering multiple biological scenarios, management objectives, and harvest strategies has the advantage of clearly representing scientific uncertainty and providing management authorities with detailed information against which their goals can be evaluated. However, it does not lead to recommendation of a specific management strategy because that would require identifying a specific management objective, which to date has not occurred for the SH subpopulation. To evaluate the biological risks of harvest, we suggest initially orienting toward Scenario 2 at a moderate degree of risk tolerance with respect to Management

Objective 1. This would suggest female harvest rates in the vicinity of h = 0.02-0.03, which correspond to starting harvest levels of 8-12 female bears/year. This is equivalent to a total (i.e., female and male) harvest rate of approximately 2.0-3.0% assuming a 1:1 male-to-female ratio in the harvest or approximately 3.0-4.5% assuming a 2:1 male-to-female ratio.

The female harvest rate is the primary determinant of whether a given harvest strategy is sustainable, because female bears are most important to population growth (Eberhardt 1990). Based on previous studies of sex-selective harvest (Taylor et al. 2008; Regehr et al. 2017b) we suggest that a female harvest rate in the range 0.02-0.03 together with a 2:1 male-to-female ratio would be unlikely to deplete males in the SH subpopulation, provided that the female harvest rate was indeed below maximum sustainable yield with respect to the female segment of the subpopulation (Taylor et al. 2008; Regehr et al. 2017b). However, we were not able to directly evaluate the biological effects of a sex-selective harvest because analyses in this report were limited to female bears only. This was necessary because aerial surveys, the primary study method for the SH subpopulation in the past decade, can provide accurate estimates of total abundance but do not provide the data on subpopulation composition or vital rates needed to model the females and males together.

The mid-range harvest strategies indicated above likely have the benefit of limiting lost opportunities for subsistence use if conditions are more like Scenario 1, while reducing the chances of severe overexploitation if conditions are more like Scenario 3a. Working from the starting point of a female harvest rate in the range 0.02-0.03, the information provided in this report can help the management authorities weigh the pros and cons of lower and higher harvests in terms of biological risk, opportunities for use, and other considerations (e.g., human safety). Furthermore, comparing future demographic data for the SH subpopulation against the biological scenarios in this report may help understand how habitat loss is affecting the subpopulation and, by extension, which scenario is most relevant to management.

All harvest strategies in this report follow a “state-dependent” harvest management approach (Regehr et al. 2017b), which is similar to the “adaptive management” approach recommended by the Polar Bear Range States (2015). State-dependent management means

that harvest levels do not remain constant into the future, but rather are updated periodically using new data from scientific studies or other sources on the current status (i.e., "state") of the subpopulation. This requires a coupled research-management framework and accurate harvest monitoring. Specifically, our analyses assumed that new aerial surveys will be completed every 5 years with a level of precision similar to the surveys in 2012 and 2016 (Obbard et al. 2015, 2018). If there is uncertainty in the ability to implement state-dependent harvest management with these conditions, a more conservative approach to harvest (i.e., a lower allowable harvest) will be necessary to mitigate risk.

Our findings should be interpreted with caution due to limited demographic data for the SH subpopulation, incomplete understanding of how sea-ice loss affects polar bear population dynamics, and use of a relatively simple demographic model that did not include male bears or a detailed mechanism of reproduction. Our modeling approach did not make purposefully conservative assumptions regarding the effects of harvest or climate change. Furthermore, the TWG received limited guidance from the responsible management authorities with respect to management objectives or risk tolerance. In the main report, we discuss several potential ways to mitigate the biological risks associated with human-caused removals. These include research and monitoring approaches to address data gaps for the SH subpopulation, and the concept of a multi-level system under which graduated management and conservation actions are tied to pre-established subpopulation thresholds.

Introduction

Management of wildlife populations often requires knowledge of demographic parameters together with a model that represents population processes and is designed to address questions of interest to management authorities (Williams et al. 2002). Most of the world's 19 polar bear (*Ursus maritimus*) subpopulations experience some level of direct human-caused mortality either through a subsistence harvest (Shadbolt et al. 2012; Laidre et al. 2015) or associated with human-bear conflicts, industrial development, or other human activities (e.g., Dyck 2006; Wilder et al. 2017). In recent decades, a primary objective of polar bear

management has been to estimate the sustainable level of human-caused removals (i.e., the number of bears that can be removed annually while meeting biological management objectives). Methods to do this have included application of a 4.5% harvest rate at a 2:1 male-to-female sex ratio, which early demographic modeling suggested was sustainable under favorable environmental conditions (Taylor et al. 1987); predictive modeling using subpopulation-specific estimates of vital rates (e.g., reproduction and survival) in a stochastic population model (e.g., RISKMAN; Taylor et al. 2006); and application of matrix-based projection models in a state-dependent (i.e., dependent on current conditions) management framework (Regehr et al. 2017b).

We present a provisional harvest risk assessment for the Southern Hudson Bay (SH) polar bear subpopulation, which used a custom demographic model and was developed to evaluate potential responses to different environmental conditions and management interventions. In the model, population processes are represented by a discrete version of the theta-logistic equation, which has been widely used to evaluate sustainable harvest of wildlife (e.g., Johnson et al. 2018). We selected the theta-logistic equation for several reasons. First, it has a simple structure that is consistent with the limited demographic information available for the SH subpopulation. Second, it can represent nonlinear density-dependent effects (Ross 2009) in a manner that is broadly consistent with the more detailed model of Regehr et al. (2017b). Third, it can accommodate variation in environmental carrying capacity (K) and intrinsic growth rate (r) resulting from habitat change or other factors. Finally, previous studies have suggested a value of theta (θ), a parameter in the theta-logistic equation that determines the relationship between population density and population growth that results in plausible demographic behaviors for polar bears (USFWS 2016). To the extent possible, our goal was to incorporate key features of the demographic model described in Regehr et al. (2017b) in a simpler model that takes advantage of available data for the SH subpopulation and could be completed under a timeline determined by management needs.

We use the demographic model to project simulated polar bear subpopulations forward in time under different biological and management conditions. In recent decades, loss of sea ice due to climate change has been implicated in declining body condition for SH polar bears

(Obbard et al. 2016). In the adjacent Western Hudson Bay subpopulation, similar declines in body condition were detected prior to declines in reproduction, survival, and abundance (Stirling et al. 1999; Regehr et al. 2007; Lunn et al. 2016; Sciullo et al. 2016). In the harvest risk assessment, we consider both density-dependent changes in K and density-independent changes in r_{max} because the mechanisms through which habitat loss affects a subpopulation can influence its ability to support harvest. Uncertainty in the demographic status of the SH subpopulation was accounted for in two ways. First, we used a Bayesian Monte Carlo approach to population reconstruction to estimate parameters of the theta-logistic equation, and then performed simulations using the full posterior distributions. Second, we developed three biological scenarios representing a plausible range of conditions for the future status of the SH subpopulation, from optimistic to pessimistic.

Our analyses use a state-dependent harvest management framework, which is similar to the "adaptive management" framework recommended by the Polar Bear Range States (2015). State-dependent management means that harvest levels do not remain constant into the future, but rather are updated periodically using new data from scientific studies or other sources on the current status (i.e., "state") of the subpopulation (Lyons et al. 2008). This can be an effective way to reduce the risk of overharvest while maintaining opportunities for use. A consequence of this approach, however, is that all findings are conditional on the existence of a coupled research-management system and accurate harvest reporting. Not following a state-dependent approach could invalidate the results, increase the chances of overexploitation, and consequently have negative implications for the SH subpopulation.

Our objectives were to: (1) develop a demographic model for the SH polar bear subpopulation that can be used to explore the probabilities of various subpopulation outcomes to a range of harvest levels; (2) develop a procedure to estimate model parameters from available data, (3) validate the model (e.g., ensure it can reproduce plausible behaviors for the subpopulation in recent decades), (4) take into account key uncertainties in demographic information, environmental conditions, and the mechanisms of subpopulation change, and (5) perform a quantitative harvest risk assessment. Results are presented as a series of potential harvest strategies and the associated probabilities of meeting several management objectives.

We took this approach because the TWG was directed to formulate management objectives, risk tolerances (i.e., acceptable probabilities of meeting management objectives), and harvest strategies with limited input from the management authorities and end users. Our findings are intended to inform prospective management actions in conjunction with other sources of information and considerations.

Methods

Abbreviations, parameters, and indexing definitions are listed in Table 1.

Data for the Southern Hudson Bay polar bear subpopulation

This section describes demographic and harvest data for the SH subpopulation that were used to develop the demographic model, estimate model parameters, and inform forward projections to evaluate harvest risk. For some data types, we only focused on females because they are the most important contributors to population growth (Eberhardt 1990) and because the demographic model did not include male bears (see section "Theta-logistic demographic model").

Harvest data

Harvest year *t* was defined as the period between 01 July of calendar year *t*-1 and 30 June of calendar year *t*. In the demographic model, annual timesteps were defined as occurring from autumn of calendar year *t* to autumn of calendar year *t*+1, to coincide with autumn-based sampling of the subpopulation during research. During subpopulation projections, the annual timestep starting in the autumn of calendar year *t* was affected by removals that occurred in the harvest year *t*+1. We did not account for the temporal offset between harvest years and annual timesteps because this would have required recompiling the harvest data and we believed that it was unlikely to affect the results.

In this report, “harvest” refers to all human-caused removals (e.g., subsistence harvest, removal of problem bears, other direct human-caused mortalities) because the demographic model only evaluated the biological effects of removals. Harvest data for some jurisdictions included uncertainty due to incomplete or inaccurate reporting. We incorporated uncertainty by treating annual harvest numbers as random variables reflecting the reported harvest levels and estimates of harvest reporting probability based on the expert opinion of regional biologists.

Harvest data for Nunavut were considered accurate and complete. For harvest years 1985-2016, the mean female harvest level was 7.8 bears/year (standard deviation (sd) of annual mean values = 2.6 bears/year). The mean proportion of females in the harvest was 0.32.

We assumed that the reported harvest in Québec was incomplete, with reporting probability represented by a uniform distribution with a minimum of 0.5 and a maximum of 0.9. The annual proportion of females in the Québec harvest was set to 0.34 based on the mean proportion of females in the reported harvest. For harvest years 1985-2016, the resulting mean female harvest level was 8.8 bears/year (sd of annual mean values = 7.4 bears/year). The mean coefficient of variation (CV) of annual harvest levels, which results from uncertainty in reporting probability, was approximately 0.37. It is possible that harvest reporting in Québec was positively correlated with the market price of polar bear hides (e.g., that reporting probability was higher in years with higher prices), but we did not have sufficient evidence to model such a relationship.

We assumed that harvest reporting in Ontario was complete 1985-1990, and that harvest was under-reported by 0-2 bears per year 1991-2016. The number of unreported bears was represented as a multinomial distribution with equal probabilities for each value. The annual proportion of females in the Ontario harvest was set to 0.30 based on the mean proportion of females in the reported harvest. For harvest years 1985-2016, the mean female harvest level was 2.7 bears/year (sd of annual mean values = 2.1 bears/year). The mean CV of annual harvest levels was approximately 0.65.

Abundance

Estimates of abundance (*N*) for the SH subpopulation were available for the periods 1984-1986 and 2003-2005 from capture-recapture studies (Kolenosky et al. 1992, Obbard et al. 2007), and for the years 2012 and 2016 from aerial surveys (Obbard et al. 2015, 2018). Some estimates were modified to minimize differences in study methods and geographic sampling area, as described below.

Mean estimates of *N* from Obbard et al. (2007) were 641 (95% CI = 401-881) for 1984-1986 and 681 (95% CI = 401-961) for 2003-2005. For convenience, we refer to these estimates as applying to 1986 and 2005, respectively. The estimates were obtained from capture-recapture studies performed in autumn in an onshore area extending from approximately the Ontario-Manitoba border to Hook Point on James Bay. We assumed that estimates of *N* for 1986 and 2005 followed normal distributions and adjusted them in two ways to increase their compatibility with abundance estimates from the aerial surveys in 2012 and 2016. First, we accounted for bears on Akimiski Island and the Twin Islands, which were not sampled during capture-recapture studies, by adding a random number of bears selected with equal probability from a lognormal distribution with approximate mean = 110 and 95% CI = 75-195, or a lognormal distribution with approximate mean = 71 and 95% CI = 57-120. These two distributions are from closed-population capture-recapture studies performed in 1997 and 1998. Obbard et al. (2007) suggested these values should be added to their estimates, to estimate the total size of the SH subpopulation. Second, we accounted for bears on small islands of James Bay and islands in eastern Hudson Bay by adding the mean number of bears in these areas based on aerial surveys conducted in 2012 and 2016. In 2012, we assumed that there were 25 bears on the small islands of James Bay (i.e., excluding Akimiski Island and the Twin Islands), 44 bears on islands in eastern Hudson Bay, and 2 bears on the Belcher Islands. These values were based on raw data from the 2012 aerial survey (Obbard et al. 2015). In 2016, we assumed that there were 13 bears on the small islands of James Bay and 53 bears on islands in eastern Hudson Bay, including Belcher Islands. These values were based on the number of observed clusters, cluster size, and detection probability from the 2016 aerial survey (Obbard et

al. 2018). Together, these calculations suggested that the mean number of bears located on small islands in James Bay and on islands in eastern Hudson Bay was approximately 69.

The estimate of *N* for 2012, obtained from a distance sampling aerial survey performed in 2011 and 2012 (Obbard et al. 2015), was assumed to follow a lognormal distribution with approximate mean = 943 and standard error (se) = 174. The estimate of *N* for 2016, obtained from a distance sampling aerial survey in 2016 (Obbard et al. 2018), was assumed to follow a lognormal distribution with approximate mean = 780 and se = 111.

As our analyses considered only female bears, we required estimates of the sex composition of the SH subpopulation. For 1986 and 2005 we estimated the proportion of females to be 0.46 and 0.57, respectively, by applying a Horvitz-Thompson estimator to model-averaged estimates of sex-specific recapture probability from Obbard et al. (2007). Since that the sex composition obtained from the subsequent aerial surveys (Obbard et al. 2015, 2018) was considered uncertain and potentially biased by the easier detection of males, we subjectively assumed that the proportion of females in 2012 and 2016 was 0.50. This lower proportion of females compared to the 2005 estimate (0.57) was also consistent with an apparent decline in the proportion of females observed between the 2012 and 2016 surveys, despite the uncertainties mentioned above regarding sex data obtained from those aerial surveys.

Abundance estimates for 1986 and 2005 were derived from an open-population capture-recapture study and therefore represent the “superpopulation”, defined as all animals with a non-negligible probability of occurring within the sampling area (Obbard et al. 2007). If bears commonly moved between the capture-recapture sampling area and the small islands of James Bay and the islands in eastern Hudson Bay, estimates of superpopulation size would likely include all animals of biological interest in the SH subpopulation and thus not require the post hoc adjustments described above. However, detailed analyses of polar bear movements among areas (e.g., using satellite telemetry data) were not available. We explored the ramifications of this uncertainty by performing a limited number of analyses with estimates of

N for 1986 and 2005 that did, and did not, include adjustments for the small islands of James Bay and the islands in eastern Hudson Bay.

Population growth rate

We used published estimates of vital rates (e.g., reproduction and survival) together with a stage-structured matrix population model (Regehr et al. 2017b) to estimate asymptotic growth rates for the SH subpopulation in the years 1986 and 2005. Survival estimates were obtained from Obbard et al. (2007, 2010). Reproductive estimates for 1986 and 2005 were obtained from Kolenosky et al. (1994) and Obbard et al. (2010), respectively. We accounted for statistical uncertainty by generating 10,000 random samples of the vital rates based on the reported means and variances, a correlation matrix for survival estimates from the most supported model in Obbard et al. (2007), and the assumption of no correlation between survival and reproduction.

First, we calculated the observed intrinsic growth rate (r_{obs}) using estimates of total survival directly from Obbard et al. (2007), which include harvest mortality. Second, we calculated potential growth rate in the absence of harvest (r_{pot}) by converting estimates of total survival (S^{total}) to estimates of un-harvested survival (*S*) using the formula:

$$S = S^{total}/(1 - H/N), \quad \text{[eqn 1]}$$

where *H* is the number of bears removed by humans and *N* is abundance. Thus, *H*/*N* is the harvest mortality rate. This approach assumes that human-caused mortality is additive within a given year, whereas density dependence in the demographic model allowed a compensatory response to changes in density across years (see section "Theta-logistic demographic model"). Equation 1 was applied to sex- and age-specific estimates of survival and abundance from 1986 and 2005 (Obbard et al. 2007). We referenced the resulting estimates of r_{pot} to a subpopulation density at maximum net productivity level (*MNPL*; i.e., we set $r_{MNPL} = r_{pot}$). This reflected the assumption that the SH subpopulation has been harvested in the vicinity of maximum sustainable yield (MSY) in recent decades. We then back-calculated the approximate maximum

intrinsic growth rate (r_{max}) using the mean ratio r_{MNPL} / r_{max} = 0.82 that has been suggested for polar bears (Regehr et al. 2017b).

Proxy for environmental carrying capacity

Changes in sea-ice habitat are expected to have demographic impacts on polar bears (e.g., Derocher et al. 2004) via density-dependent mechanisms, density-independent mechanisms, or both (Regehr et al. 2017b). In the demographic model, density-dependent effects were incorporated by using the number of ice-covered days per year, calculated using the methods of Stern and Laidre (2016), as a proxy for *K*. Each year, the sea-ice area reaches a maximum in March and a minimum in September. We defined a threshold halfway between the mean March sea-ice area and the mean September sea-ice area for the period 1979-2016. Then, we calculated the number of ice-covered days in year *t* as the total number of days before the sea-ice area drops below the threshold in spring of year *t*, and after the sea-ice area rises above the threshold in fall of year *t*. This sea-ice metric has been included in the IUCN/SSC Polar Bear Specialist Group's status table (Durner et al. 2018) and used in other harvest risk assessments (Regehr et al. 2017a, 2018a).

We represented future trends and variability in *K* by projecting the number of ice-covered days forward in time using linear models and the methods of Gelman and Hill (2007) to simulate uncertainty in the slope and residual standard errors. Projected values of ice-covered days in years t = 2, 3, … T were standardized by dividing by the fitted value at the start of projections (year t = 1). This resulted in a dimensionless parameter (κ) representing proportional changes in *K*. During population projections, carrying capacity at year *t*, calculated as $K_t = K_{t=1} \times \kappa_t$, operated on population growth through the theta-logistic model (see section "Theta-logistic demographic model"). In some analyses we used an alternative, nonlinear method to project *K* forward in time (see section "Simulations to evaluate harvest risk").

Demographic model

We constructed a demographic model based on the theta-logistic equation, which is widely used in population ecology for species with nonlinear negative density dependence (e.g., Saether et al. 2002). We modeled the female component of the SH subpopulation only because the theta-logistic equation does not include sex or age structure. Therefore, the model is not capable of representing the complex life cycle of polar bears (e.g., polygynous reproduction and extended maternal care) or the demographic effects of changes in population composition (e.g., a skewed sex ratio due to sex-selective harvest).

Model description

The theta-logistic equation can be written as follows:

$$N_{t+1} = N_t \times \left\{ 1 + \left[r_{max} \left(1 - \left(\frac{N_t}{K} \right)^{\theta} \right) \right] \right\} - hN_t, \qquad \text{[eqn2]}$$

where N is abundance, r_{max} is maximum intrinsic growth rate, K is environmental carrying capacity, h is the harvest rate (i.e., the percentage of subpopulation abundance removed), and θ is a shape parameter that determines how the growth rate changes as a function of subpopulation density. The product hN_t is the harvest level (H_t; the number of bears removed from the population between timesteps t and t+1). The notation t indicates parameters that can change across annual timesteps (i.e., t = 1, 2, 3…, T). For simplicity, equation 2 is written with temporal notation only for N. In practice, the model can include temporal variation in K, r_{max}, and H. For all subpopulation projections, we fixed the density-dependent shape parameter to θ = 5.045 because this value produces demographic behaviors consistent with other models for polar bears (USFWS 2016). Data were not available to estimate a value of ϑ specific to the SH subpopulation.

Key behaviors of a theta-logistic model can be demonstrated by growth and yield curves (Figures 1 and 2, respectively). These curves were generated using r_{max} = 0.06, a typical value for polar bears (Regehr et al. 2017b). At low densities (i.e., small N/K) the observed growth rate

is equal to the maximum intrinsic growth rate (r_{max}) because crowding and competition are at a minimum (Figure 1). Furthermore, the observed growth rate remains high until *N* starts to approach *K*, at which point growth declines rapidly until stability is reached at an equilibrium abundance $N = K$. This nonlinear density dependence results in an asymmetric yield curve for which *MSY* occurs at approximately $MNPL = 0.7K$ (Figure 2). The corresponding ratio r_{MNPL} / r_{max} is approximately 0.83, suggesting relatively strong compensation for human-caused mortality. These demographic behaviors are broadly consistent with those resulting from a stage-structure matrix population model based on the polar bear life cycle (Regehr et al. 2015, 2017b). It is important to use a biologically realistic model of density dependence when evaluating the combined effects of habitat change and human-caused removals (Guthery and Shaw 2013; Williams 2013).

Mechanisms of population change

Environmental change can affect wildlife populations through density-dependent and density-independent mechanisms (e.g., Winship and Trites 2006). Negative density-dependent effects can be thought of as declines in habitat quantity, which lead to a reduction in the number of animals that an environment can support (i.e., reduced *K*). Negative density-independent effects can be thought of as declines in habitat quality, which lead to a reduced capacity for population growth regardless of the number of animals (i.e., reduced r_{max}). Depending on the type of habitat change and the ecology of the species, the parameters r_{max} and *K* could be mechanistically linked such that they change in unison. These and other concepts in population dynamics and harvest management for polar bears are reviewed in Appendix C of USFWS (2016). In the current report, the theta-logistic model could accommodate density-dependent effects through changes in *K*, density-independent effects through changes in r_{max}, and combined effects through independent changes in both parameters (Figure 2).

Management framework

State-dependent harvest

Regehr et al. (2017b) described a state-dependent harvest management framework under which the harvest level is periodically updated using new information on subpopulation abundance and growth rate. The current harvest risk assessment included a simplified state-dependent framework that used new estimates of *N* to update harvest level but did not use new estimates of r_{max} to update the harvest rate. For a given harvest strategy, the harvest level at each time step *t* was calculated as follows:

$$H_t = h \times \widetilde{N}_t \,, \qquad \text{[eqn 3]}$$

where *H* is the number of females removed; *h* is a target harvest rate, defined as the proportion of female bears to be removed by humans each year; and $\widetilde{N}$ is an estimate of female abundance selected as the 50th percentile of its sampling distribution.

A state-dependent harvest management approach requires specifying the management interval, defined as the number of years between successive subpopulation assessments and changes to the harvest based on updated demographic information. We used a management interval of 5 years. During simulated subpopulation assessments, the estimate of *N* in year *t* was randomly selected from a normal distribution with a mean equal to the average abundance in years *t*-3, *t*-2, and *t*-1 and a standard deviation based on CV($\widetilde{N}$) = 0.16. This is the mean CV from the 2012 and 2016 aerial surveys (Obbard et al. 2015, 2018), reflecting the assumption that future subpopulation assessments will produce estimates of *N* with a similar level of precision.

Management objectives and risk tolerance

Evaluating harvest strategies requires statements of the biological outcomes that managers want to achieve. In this report we evaluated harvest relative to the following three management objectives.

- Management Objective 1: Maintain a harvested subpopulation at an equilibrium size greater than *MNPL*. During stochastic projections, the probability that subpopulation abundance was greater than *MNPL* at time step *t* was denoted $P_t^{N>MNPL}$. To calculate $P_t^{N>MNPL}$ we used a single value of *MNPL* corresponding to a relative density N/K = 0.70, which is similar to the mean estimate of relative density at *MNPL* across a wide range of vital rates (Regehr et al. 2017b). This provided a consistent point of reference for evaluating harvest effects across different biological and environmental conditions.
- Management Objective 2: Maintain a harvested subpopulation at an equilibrium size greater than 90% of starting subpopulation size (i.e., subpopulation size at year *t* = 1). The probability of meeting Management Objective 2 at time step *t* was denoted $P_t^{N>0.9N1}$.
- Management Objective 3: Maintain a harvested subpopulation at an equilibrium size above a minimum threshold, below which the function and viability of the subpopulation would be compromised. The probability of meeting Management Objective 3 at time step *t* was denoted $P_t^{N>threshold}$. In the current report, we calculated $P_t^{N>thresh}$ based on a threshold of 175 female bears.

These or similar objectives are common indices of sustainability in wildlife management (Sutherland 2001) and have been used in other risk assessments for polar bears (Regehr et al. 2018a). Assessing whether a given harvest strategy meets a management objective requires a statement of risk tolerance, which specifies the required probability of meeting the objective. Because management authorities for the SH subpopulation did not provide specific guidance on acceptable amounts of risk, we present results for a wide range of harvest strategies rather than for a smaller number of strategies corresponding to pre-specified levels of risk tolerance. As a point of reference, we note that previous harvest risk assessments for polar bears using Management Objective 1 have defined "low" risk tolerance as $P_t^{N>MNPL}$ > 0.90 and "medium" risk tolerance as $P_t^{N>MNPL}$ > 0.70 (Regehr et al. 2017a, 2018a). The same levels of risk tolerance

should not be applied to all three alternative management objectives because the consequence of failing to meet each objective is different.

Steps for population reconstruction

We used population reconstruction to estimate parameters of the theta-logistic model that provided a good fit to empirical demographic data for the SH subpopulation. This ensured that the demographic model could reproduce the SH subpopulation's historic status and trend. Also, it provided estimates of model parameters to use in forward projections. We present general methods here and provide additional details in the section "Simulations to evaluate harvest risk".

Population reconstruction was performed using a Bayesian Monte Carlo approach. First, we specified prior distributions for r_{max} and $N_{t=1}/K_{t=1}$ based on existing knowledge of polar bear demography and assumptions that were specific to each biological scenario. Second, we ran retrospective projections over the period 1986-2016, or a subset of these years, using the theta-logistic model parameterized with 100,000 random samples from the prior distributions for r_{max} and $N_{t=1}/K_{t=1}$. Abundance at t = 1 was randomly selected from a uniform distribution covering the range of the empirical confidence interval for N in 1986, 2005, or 2012, depending on which year the retrospective projection started. A stochastic harvest was applied at each time step based on the historic harvest (see section "Harvest data"), and K varied stochastically from year-to-year with a trend and variance that were specific to each biological scenario. Third, for each retrospective projection we calculated a likelihood based on the probabilities of observing the selected value of r_{max} and the projected values of N, given the empirical estimates of r_{max} for 1986 and 2005 from capture-recapture studies (Obbard et al. 2007), and the empirical estimates of N for 1986, 2005, 2012, and 2016 from capture-recapture studies and aerial surveys (Obbard et al. 2015, 2018). Sets of model parameters that had a value of r_{max} or a projected value of N with zero probability resulted in a log-likelihood of negative infinity, and thus were discarded. The remaining sets of model parameters, with their normalized likelihood values considered to be observation weights, were used to generate empirical probability

density functions for r_{max} and starting $N_{t=1}/K_{t=1}$, which in turn were used to generate posterior distributions. Unless otherwise noted, all reconstructions used estimates of *N* for 1986 and 2005 that had been adjusted for bear on small islands in James Bay and in eastern Hudson Bay.

Steps for subpopulation projections

We used the theta-logistic model to project simulated polar bear subpopulations forward in time. At each time step, harvest was applied using equation 3, after which the subpopulation was projected forward one year using equation 2. Forward projections were run for 35 years, which is approximately three polar bear generations (Regehr et al. 2016). Three species-specific generation lengths is a common timeframe for conservation assessments because it scales with life history processes (Mace et al. 2008) and, for our purposes, allowed assessment of relatively long-term harvest effects.

For a given projection it was necessary to specify biological parameters of the subpopulation, environmental conditions and how they influenced biological parameters, and a harvest strategy. The relevant biological parameters were $N_{t=1}$, r_{max}, and starting subpopulation density relative to carrying capacity (i.e., $N_{t=1}/K_{t=1}$, which together with $N_{t=1}$ permits calculation of $K_{t=1}$). Environmental conditions included temporal changes in *K*, temporal changes in r_{max}, or both. Harvest strategies were defined by a time-constant harvest rate (*h*). The annual harvest level during the first management interval (i.e., for years t = 1, 2, 3, 4, 5) was calculated based on the empirical point estimate of female abundance in 2016 (Obbard et al. 2018). This ensured that starting harvest levels were based on the best-available information and were consistent across projections with the same harvest strategy. At the beginning of subsequent management intervals, the harvest level was calculated using equation 3 with a value of $\widetilde{N}$ derived from a simulated subpopulation assessment.

To reflect key sources of uncertainty we performed stochastic projections over which certain parameters varied. We define a “simulation” as 10,000 forward projections that used the same biological parameters, method to project *K* and specify temporal variation in r_{max}, and harvest strategy. Within a simulation, sampling variation (i.e., statistical uncertainty in

demographic information) was incorporated by selecting 10,000 random samples of the theta-logistic model parameters from their posterior distributions (see section "Population reconstruction"). Environmental variation was incorporated by using a different stochastic projection of *K* for each sample of model parameters (see section "Proxy for environmental carrying capacity"). For each simulation we recorded the probabilities of meeting the three management objectives as well as the following subpopulation outcomes.

- $\overline{N}_t$: Mean subpopulation abundance (female bears) at time step *t*.
- $\overline{K}_t$: Mean environmental carrying capacity (female bears) at time step *t*.
- $\overline{H}_t$: Mean annual harvest level (female bears/year) at time step *t*. For a given fixed-rate harvest strategy, the harvest level can change over time if *N* changes due to habitat change or the effects of harvest.
- P_{ext}: Probability of extirpation, defined as *N* falling below a quasi-extinction threshold of 15% of starting *N*. Subpopulations that crossed below the quasi-extinction threshold at any time step were considered extirpated and could not recover.

Simulations to evaluate harvest effects

We developed three biological scenarios to represent plausible alternatives, from optimistic to pessimistic, for the status of SH subpopulation. Each scenario used a different approach to population reconstruction and made different assumptions about future environmental conditions. For each scenario, we performed 17 simulations corresponding to female harvest rates from 0-8% in 0.5% increments.

<u>Scenario 1</u>

This optimistic scenario reflected the hypothesis that the future status of the SH subpopulation will be similar to its status 1986-2016, during which the subpopulation was capable of strong growth and the long-term trend in abundance was approximately stable.

Population reconstruction was performed for the period 1986-2016 using estimates of r_{max} from 1986 and 2005, estimates of *N* from 1986, 2005, 2012, and 2016, and the observed harvest. The prior for r_{max} was a normal distribution with a mean of 0.06 and a standard deviation of 0.02, which is the approximate distribution of point estimates of r_{max} from case studies for polar bears as reviewed in Regehr et al. (2017b). Use of this prior represents the hypothesis that the capacity for growth of the SH subpopulation during the period 1986-2016 was similar to that of other polar bear subpopulations in recent decades. The prior for $N_{t=1}/K_{t=1}$ was a uniform distribution with a minimum of 0.5 and maximum of 0.9. Regehr et al. (2017b) suggested that a mean equilibrium density of $N/K \approx 0.70$ corresponded to *MNPL* across a wide range of vital rates for polar bears. We used a diffuse uniform distribution with a mean of 0.70 because, although the subpopulation density for 1986 is not known, it was reasonable to assume that the SH subpopulation had been harvested in the general vicinity of MSY in the years prior to 1986. Population reconstruction was performed using stochastic projections of *K* with the variance based on a linear model fit to the time-series of ice-covered days 1979-2016, and the slope set to 0. We set the slope to 0 because, on average, a stable carrying capacity seemed consistent with the relatively stable estimates of *N* for the period 1986-2016. During forward projections for Scenario 1, *K* was projected using the estimated variance and slope from a linear model fit to the sea-ice data 1979-2016. This reflected the hypothesis that the SH subpopulation will experience gradual density-dependent declines in *K* (approximately 3% per decade) in proportion to the observed decline in the number of ice-covered days per year in the SH management area. Forward projections for Scenarios 1 used time-constant values of r_{max}, reflecting the hypothesis that the SH subpopulation will not experience density-independent limitation due to habitat change.

Scenario 2

This middle-of-the-road scenario reflected the hypothesis that the future status of the SH subpopulation will be similar to its status 2005-2016, during which the subpopulation was

capable of moderate growth and may have experienced a decline in abundance toward the end.

Population reconstruction was performed for the period 2005-2016 using the estimate of r_{max} from 2005, estimates of N from 2005, 2012, and 2016, and the observed harvest. The priors for r_{max} and $N_{t=1}/K_{t=1}$ were the same as for Scenario 1. During population reconstruction we used stochastic projections of K with the estimated variance and slope from a linear model fit to the sea-ice data 1979-2016. This reflected the hypothesis that the SH subpopulation experienced gradual density-dependent declines in K during the period 2005-2016. We also specified a deterministic decline in r_{max} equivalent to 3% of its starting value per decade. This reflected the hypothesis that the SH subpopulation also experienced gradual density-independent declines in proportion to declining sea ice. For Scenario 2, forward projections used the same temporal patterns in K and r_{max} as the population reconstruction. This reflected the hypothesis that the SH subpopulation will continue to experience gradual declines that are both density dependent and density independent.

Scenario 3

This pessimistic set of scenarios reflected the hypothesis that the future status of the SH subpopulation will be similar to its status 2012-2016, during which subpopulation abundance likely declined. Scenarios 3a and 3b attribute the decline to density-independent and density-dependent mechanisms, respectively. This distinction is important because the mechanisms of subpopulation change influence the ability to support harvest.

Scenario 3a

Population reconstruction was performed for the period 2012-2016 using estimates of N from 2012 and 2016, and the observed harvest. The prior for r_{max} was a uniform distribution with a maximum of 0.06 and a minimum of 0, reflecting the hypothesis that the SH subpopulation was undergoing below-average growth compared to other polar bear

subpopulations. The prior for $N_{t=1}/K_{t=1}$ was the same as for scenarios 1 and 2, and both the population reconstruction and forward projections used the same temporal changes in K and r_{max} as Scenario 2. Scenario 3a reflected the hypothesis that the SH subpopulation experienced strong density-independent limitation prior to 2016, and will continue to experience gradual declines that are both density dependent and density independent.

Scenario 3b

Population reconstruction was identical to Scenario 1 with one exception. Whereas Scenario 1 assumed stability in K, Scenario 3b included a nonlinear decline in K over the period 1986-2016 that continued into forward projections. Specifically, during population reconstruction we used a logistic function to model K. In addition to $K_{t=1}$, which was specified in the same manner as for other scenarios, the logistic function required a parameter representing the year in which K changed most rapidly (i.e., the x-axis location of the midpoint of the logistic function's sigmoidal curve) and a parameter specifying the steepness of the curve. These two parameters were estimated using noninformative priors and the same Bayesian Monte Carlo approach described above. Scenario 3b reflected the hypothesis that the SH subpopulation would remain capable of strong growth if habitat were sufficient, but that the subpopulation will experience severe density-dependent declines in K that represent a collapse in the region's ability to support polar bears.

Software

Computations were performed in the R computing language (version R 3.4.0; The R Project for Statistical Computing; http://www.r-project.org). Matrix projection models were constructed and evaluated using the packages 'popbio' (Stubben and Milligan 2007) and 'popdemo' (Stott et al. 2011).

Results

Data for the Southern Hudson Bay polar bear subpopulation

Our analyses used a combination of published, unpublished, and derived demographic data for the SH polar bear subpopulation. Female harvest was estimated by summing stochastic harvest levels for Nunavut, Ontario, and Québec. For harvest years 1985-2016, the mean female harvest was 19.3 bears/year (sd of annual mean values = 7.9 bears/year; Figure 3). Estimates of total (i.e., female and male) abundance, and estimates of the proportion of females in the subpopulation, were obtained from capture-recapture studies (Obbard et al. 2007) and aerial surveys (Obbard et al. 2015, 2018). We present estimates of *N* from capture-recapture studies in 1986 and 2005 that were, and were not, adjusted to include bears that were potentially missed on the small islands in James Bay and the islands in eastern Hudson Bay (Table 2). For the period 1985-2016 the mean total (i.e., female and male) harvest rate for the SH subpopulation was approximately 0.07 (95% CI = 0.03-0.15). The mean female harvest rate 1985-2016, expressed as the proportion of females removed each year, was approximately 0.05 (95% CI = 0.01-0.11).

We estimated asymptotic growth rates using a matrix-based projection model parameterized with vital rates from capture-recapture studies. Estimates of observed growth rate and maximum intrinsic growth rate for 1986 were r_{obs} = 0.02 (-0.07-0.08) and r_{max} = 0.10 (0.01-0.15). Estimates for 2005 were r_{obs} = -0.02 (-0.18-0.07) and r_{max} = 0.01 (-0.17-0.13). The point estimates of r_{max} for 1986 and 2005 were near the upper and lower limits for polar bears, respectively (Regehr et al. 2017b), although precision of the estimates was low.

The number of ice-covered days in the SH management area declined significantly during the period of the satellite record (1979-2016: linear model slope = -0.63 ice-covered days/year; se[slope] = 0.21, $P < 0.01$) and during the period of current demographic modeling (1984-2016: linear model slope = -0.76 ice-covered days/year; se[slope] = 0.29, $P = 0.01$). Ice conditions varied from year-to-year and had potentially different trends over shorter time periods (Figure 4). Similar short-term variation, including transient periods of stability in sea-ice conditions, has been documented for the adjacent Western Hudson Bay subpopulation (Lunn et

al. 2016). Stochastic projections of *K* based on a linear model fit to the sea-ice metric 1979-2016 declined by approximately 3% per decade.

Simulations to evaluate harvest risk

We used population reconstruction to estimate parameters of the theta-logistic model for three biological scenarios. For each scenario, we then performed simulations to evaluate the effects of female harvest rates from 0-8% under a state-dependent harvest management framework. In this section, we compare results across scenarios by examining harvest strategies with approximately an 80% probability of meeting Management Objective 1. We also present results for harvest strategies corresponding to a wide range of risk tolerances in table form.

Scenario 1 (optimistic)

The posterior distribution of r_{max} (Figure 5) estimated from population reconstruction had a mean of 0.08 (95% CI = 0.05-0.11). The posterior of $N_{t=1}/K_{t=1}$ had a mean of 0.73 (95% CI = 0.53-0.89). Under this scenario, the SH subpopulation was capable of strong growth 1986-2016. The population reconstruction for Scenario 1 provided a reasonable fit to historic data (Figure 6). For example, the mean value of *N* from retrospective projections was slightly above the empirical estimates of *N* in 1986 and 2016, and slightly below the empirical estimates of *N* in 2005 and 2012. To explore sensitivity of results to estimates of *N* for 1985 and 2005, we performed a supplemental population reconstruction for Scenario 1 using values of *N* that were not adjusted for bears on the small islands of James Bay and islands in eastern Hudson Bay (Table 2). The estimate of r_{max} did not change at the level of precision that we report, suggesting that this issue was unlikely to have a substantive impact on results.

Simulations for Scenario 1 indicated that a subpopulation with these characteristics could likely support a relatively high harvest (Table 3). For example, a harvest strategy with female harvest rate *h* = 0.055 resulted in $P_{t=35}^{N>MNPL}$= 0.78, which is close to an 80% probability of meeting Management Objective 1. This strategy would correspond to a starting harvest level

$\overline{H}_{t=1}$ = 21 female bears/year and a mean ending harvest level $\overline{H}_{t=35}$= 19 female bears/year, where the difference results from gradual declines in projected values of *K*. Under this harvest strategy, the subpopulation would have a low probability of crossing below the minimum abundance threshold (i.e., $P_{t=35}^{N>thresh}$= 0.99) and a negligible probability of extirpation (i.e., P_{ext} = 0.00). We report results up to a maximum female harvest rate of *h* = 0.060, because at this point the probability of crossing below the minimum abundance threshold starts to increase rapidly even for the most optimistic Scenario 1.

Scenario 2 (middle-of-the-road)

The posterior distribution of r_{max} from population reconstruction had a mean of 0.05 (95% CI = 0.02-0.09). The posterior of $N_{t=1}/K_{t=1}$ had a mean of 0.73 (95% CI = 0.51-0.90). Under this scenario, the SH subpopulation was capable of average growth 2005-2016. The population reconstruction for Scenario 2 provided a reasonable fit to historic data (Figure 7).

Simulations for Scenario 2 indicated that a subpopulation with these characteristics could likely support a moderate harvest (Table 4). For example, a harvest strategy with a female harvest rate *h* = 0.025 resulted in $P_{t=35}^{N>MNPL}$= 0.84. This strategy would correspond to a starting harvest level $\overline{H}_{t=1}$ = 10 female bears/year and a mean ending harvest level $\overline{H}_{t=35}$= 10 female bears/year. Under this strategy, the subpopulation would have a low probability of crossing below the minimum threshold (i.e., $P_{t=35}^{N>thresh}$= 0.99) and a negligible probability of extirpation (i.e., P_{ext} = 0.00).

Scenario 3 (pessimistic)

For Scenario 3a the posterior distribution of r_{max} from population reconstruction had a mean of 0.03 (95% CI = 0.00-0.06), which was similar to its prior. The posterior of $N_{t=1}/K_{t=1}$ had a mean of 0.71 (95% CI = 0.51-0.90). Under this scenario, the SH subpopulation was capable of limited growth 2005-2016. The population reconstruction for Scenario 3a provided a reasonable fit to historic data (Figure 8).

Simulations for Scenario 3a indicated that a subpopulation with these characteristics could support a low harvest (Table 5). For example, a harvest strategy with *h* = 0.01 resulted in $P_{t=35}^{N>MNPL}$= 0.79. This strategy would correspond to a starting harvest level $\overline{H}_{t=1}$ = 4 female bears/year and a mean ending harvest level $\overline{H}_{t=35}$= 4 female bears/year. Under this harvest strategy, the subpopulation would have a negligible probability of crossing below the minimum threshold (i.e., $P_{t=35}^{N>thresh}$= 1.0) and a negligible probability of extirpation (i.e., P_{ext} = 0.00).

For Scenario 3b the posterior distribution of r_{max} from population reconstruction had a mean of 0.08 (95% CI = 0.05-0.11). The posterior of $N_{t=1}/K_{t=1}$ had a mean of 0.73 (95% CI = 0.51-0.91). Under this scenario, the SH subpopulation was capable of strong growth 1986-2016. The population reconstruction for Scenario 3b provided a reasonable fit to historic data (Figure 9).

Although retrospective projections for Scenario 3b (Figure 9) appear similar to those for Scenario 1 (Figure 6), the key difference is that *K* was represented by a logistic function and started to decline rapidly in the mid-2000s under Scenario 3b, whereas *K* remained stable until 2016 and declined only gradually after that under Scenario 1. For Scenario 3b the estimated location of the logistic curve's midpoint was timestep *t* = 24 (95% CI = 8-42) of forward projections, which corresponds to the year 2039. The estimated steepness parameter in the logistic function was -0.22 (95% CI = -0.40 to -0.04).

Simulations for Scenario 3b indicated that a subpopulation with these characteristics would be relatively insensitive to harvest (Table 6). Because r_{max} remained high, the subpopulation maintained its ability to compensate for human-caused removals through reduced negative density effects. Furthermore, a collapsing *K* made extirpation unavoidable regardless of human-caused removals. These dynamics are best demonstrated by visualizing forward projections for Scenario 3b with no harvest (Figure 10a) and with *h* = 0.055 (Figure 10b). The two trajectories are nearly parallel because, when the effects of habitat loss are density dependent, it is possible to maintain *N* slightly below a declining K without accelerating subpopulation declines. Note that, in Figure 10, individual trajectories that decline from a relatively high *N* (e.g., 200 bears) to *N* = 0 in one timestep are a consequence of strongly negative growth rates when *K* is declining rapidly and r_{max} is large. This phenomenon is, to some

extent, a mathematical idiosyncrasy of the theta-logistic equation. Nonetheless, Scenario 3b demonstrates that a rapid and unidirectional collapse in *K* could result in a high probability of extirpation that is minimally influenced by harvest. This is different from Scenario 3a, under which the probability of extirpation was negligible in the absence of harvest and increased rapidly at higher harvest rates.

Discussion

This report presents a provisional harvest risk assessment for the SH polar bear subpopulation. The assessment was based on a custom demographic model that has a structure consistent with the available data and was able to reproduce recent trends for the SH subpopulation. During forward projections the model incorporated the potential effects of sea-ice loss due to climate change, a primary threat to polar bears throughout much of their range (Atwood et al. 2016; Regehr et al. 2016). The final results are a series of potential harvest strategies and their estimated effects. Results are presented for several plausible biological scenarios due to uncertainty in the current and future status of the subpopulation.

Demographic status of the Southern Hudson Bay polar bear subpopulation

Recent demographic data for the SH subpopulation are primarily from capture-recapture studies in the 1980s and 2000s (Obbard et al. 2007) and two aerial surveys in the 2010s (Obbard et al. 2015, 2018). Assessing trends in abundance is complicated by differences in the geographic distribution of sampling effort and in the definition of the study population for capture-recapture studies and aerial surveys. Although we adjusted estimates of *N* to improve consistency between the study types this may not have been accurate due to lack of information on subpopulation composition and animal movements. We conclude that it is not possible to evaluate long-term trends in the size of the SH subpopulation based on published information. There is evidence of a likely decline from 943 bears in 2012 (Obbard et al. 2015) to 780 bears in 2016 (Obbard et al. 2018) based on aerial surveys that had consistent

methodology. Such a decline appears consistent with loss of sea-ice habitat due to climate change and documented declines in nutritional condition (Obbard et al. 2016). Declines in abundance estimates for the adjacent WH subpopulation during the period 2011-2016, although not statistically significant, suggest that changes in the SH subpopulation were not caused by movement of bears to the north, and that the two subpopulations may be exhibiting similar responses to broader ecosystem change (Stapleton et al. 2014; Dyck et al. 2017). However, Indigenous Knowledge does not support the conclusion of a declining SH subpopulation (Laforest et al. 2018; NMRWB 2018). This perspective, together with multiple types of scientific uncertainty about the status of the SH subpopulation, led to the development of the most optimistic Scenario 1. Furthermore, declines in the number of ice-covered days have been smaller for SH bears than for other subpopulations (Stern and Laidre 2016) and previous studies have not identified relationships between annual sea-ice conditions and vital rates or nutritional status (Obbard et al. 2007, 2016). The demographic status of the SH subpopulation is likely a function of multiple, interacting factors that operate at different time scales and cannot be resolved with the current data.

We used vital rates from Obbard et al. (2007, 2010) in a matrix-based projection model (Regehr et al. 2017b) to estimate maximum intrinsic growth rate (r_{max}) in 1986 and 2005. The estimate of r_{max} = 0.10 for the 1980s was high for polar bears, suggesting a strong capacity for growth and ability to support harvest, assuming this estimate was unbiased. In contrast, the estimate of r_{max} = 0.02 for the early 2000s was low for polar bears. This may be due to negative bias in survival estimates, which is common at the end of capture-recapture studies for mobile animals (Devineau et al. 2006; Regehr et al. 2009). Some degree of bias seems likely given that, if r_{max} were this low and did not increase after 2005, the SH subpopulation would likely have been severely overharvested in recent decades and declined to a small size. It is unknown to what extent low estimates of survival in the early 2000s reflect bias, true declines (e.g., due to habitat loss), or both. High statistical uncertainty in estimated vital rates further complicates interpretation. We note that bias in survival would suggest bias in estimates of *N* as well, because the two parameters are linked within the capture-recapture framework. This is less of

a concern, however, because mean percent relative bias of a similar magnitude (e.g., -5%) in survival and abundance have substantially different ramifications for population dynamics.

Additional insight into the status of the SH subpopulation can be gained from the harvest data. We accounted for incomplete reporting in some jurisdictions by representing harvest reporting probability as a random variable, although the accuracy of this approach cannot be confirmed. For example, we assumed that reporting probability in Québec followed a diffuse uniform distribution whereas anecdotal evidence suggests that reporting may be positively correlated with the market price of polar bear hides. Use of inaccurate harvest data during population reconstruction could lead to biased estimates of theta-logistic model parameters (see below), which in turn could influence estimates of harvest risk. Taking statistical uncertainty into account, the mean total (i.e., female and male) harvest rate of approximately 0.07 (95% CI = 0.03-0.15) for the period 1985-2016 was likely higher than the 4.5% harvest rate that been considered sustainable for polar bears at a 2:1 male-to-female ratio when environmental conditions are favorable (Taylor et al. 1987). The fact that abundance in the 2010s appeared broadly comparable to previous estimates seems consistent with other evidence that the SH subpopulation was, on average, capable of strong growth in recent decades. However, it is possible that harvest was a partial factor in declines in abundance during the period 2012-2016. Furthermore, some harvest occurs on the sea ice in spring when the SH subpopulation intermixes with the adjacent Western Hudson Bay and Foxe Basin subpopulations (Viengkone et al. 2018), meaning that some animals removed from the SH management unit are members of adjacent subpopulations. Additional data and analyses are required to understand how movements of polar bears in the Hudson Bay region affect research and management of the SH subpopulation.

Assessment of harvest effects

We evaluated harvest under several biological scenarios that were developed using different approaches to population reconstruction together with different assumptions about trends in K and r_{max}. We considered multiple scenarios because of uncertainty in the current

and future demographic status of the SH subpopulation. Unlike the adjacent Western Hudson Bay subpopulation (Lunn et al. 2016), empirical estimates of relationships between environmental conditions and subpopulation growth rate were not available. We intended the scenarios to encompass a range of plausible biological conditions, from optimistic to pessimistic. One consequence of using multiple scenarios is that multiple harvest strategies could meet management objectives, depending on which scenario is considered. Although this makes it difficult to recommend a specific harvest strategy, it has the advantage of clearly presenting scientific uncertainty in the status of the SH subpopulation and its ability to support human-caused removals. Comparing the future status of the SH subpopulation against the biological scenarios in this report may help inform how habitat loss is affecting the subpopulation and, by extension, which scenario is most relevant to management. More broadly, the analyses in this report provide a basis for quantitative and testable biological hypotheses, a key component of evidenced-based wildlife management (Houlahan et al. 2017).

Population reconstruction for Scenario 1 estimated r_{max} = 0.08, which is high compared to other case studies for polar bears (Regehr et al. 2017b). This suggests that the SH subpopulation was, on average, capable of strong growth during the period 1986-2016. Forward projections for Scenario 1 reflected this optimistic hypothesis that the status of the SH subpopulation for the next 35 years will be similar to the past 30 years, with only gradual declines in *K* proportional to projected declines in the number of ice-covered days per year in the SH management area. However, for this to be true, one must assume that the apparent decline in *N* between 2012 and 2016 was either not real or a transient phenomenon, and that continued sea-ice loss will have only minor density-dependent effects. For Scenario 1, a harvest strategy with a female harvest rate *h* = 0.055 resulted in an approximately 80% probability of meeting Management Objective 1, which was to maintain *N* above maximum net productivity level (i.e., $P_{t=35}^{N>MNPL} \approx 0.80$). This placeholder harvest strategy fell between the “low” and “medium” degrees of risk tolerance used in other studies (Regehr et al. 2017a, 2018a; see section “Management framework”) and therefore seemed reasonable for demonstration. The starting harvest level for this strategy was 21 female bears/year (Table 3), which is similar to the mean observed harvest of approximately 19 female bears/year 1986-2016. This makes sense

given the assumptions of Scenario 1 and suggests that our modeling approach can reproduce plausible behaviors for the SH subpopulation. Overall, simulations for Scenario 1 suggest that the SH subpopulation could continue to support a female harvest in the vicinity of 20 bears/year provided that environmental conditions are relatively stable, the subpopulation remains capable of strong growth, and a state-dependent harvest management framework is in place with complete harvest reporting and a 5-year management interval. Given the combined evidence for habitat loss, ecosystem change, and declining abundance for the SH subpopulation, the TWG considered Scenario 1 to be very optimistic and likely unrealistic. Therefore, we recommend that results from this scenario should not be a primary basis for management decisions.

Population reconstruction for Scenario 2 estimated r_{max} = 0.05, which is average for polar bears. This estimate was lower than for Scenario 1 because Scenario 2 used data from 2005-2016 only. This excluded the high empirical estimate of r_{max} in 1986 (Obbard et al. 2007) and placed more weight on the lower estimate of *N* in 2016 (Obbard et al. 2018). Forward projections for Scenario 2 included declines in both r_{max} and *K* in proportion to projected sea-ice declines. Scenario 2 reflected the middle-of-the-road hypothesis that the status of the SH subpopulation for the next 35 years will be similar to the past decade, during which there is some evidence of demographic declines, and that continued sea-ice loss will have gradual but progressive density-dependent and density-independent effects. For Scenario 2, a harvest strategy with *h* = 0.025 corresponded to approximately $P_{t=35}^{N>MNPL}$ = 0.80 (Table 4). The starting harvest level for this strategy was 10 female bears/year. Assuming that the proportion of females in the SH subpopulation is currently 0.50, this would correspond to a total (i.e., female and male) harvest rate of approximately 0.038, provided that harvest adheres to a 2:1 male-to-female ratio. This is slightly below the 4.5% rate at a 2:1 male-to-female ratio that has generally been considered sustainable under favorable environmental conditions. Insight can be gained by taking a harvest strategy that appears sustainable under one scenario and evaluating its potential effects under a different scenario. For example, a strategy with *h* = 0.55 was unlikely to have negative subpopulation-level effects under Scenario 1 (Table 3). However, if this strategy was applied to a subpopulation with a demographic status like Scenario 2 it could

result in a high probability of subpopulation depletion (e.g., $P_{t=35}^{N>MNPL}$= 0.17), a moderate probability of crossing below the minimum threshold ($P_{t=35}^{N>thresh}$ = 0.64), and lost opportunities for sustainable use (Table 4).

Scenario 3 included two pessimistic representations of the SH subpopulation that have different ramifications for harvest. Population reconstruction for Scenario 3a estimated r_{max} = 0.03, which is low for polar bears. This was a consequence of using a prior distribution for r_{max} with a smaller mean together with data from 2012-2016 only. Similar to Scenario 2, forward projections for Scenario 3a included projected declines in both r_{max} and *K*. Scenario 3a reflected the pessimistic hypothesis that the SH subpopulation has recently experienced, or soon will experience, strong density-independent limitation and that continued sea-ice loss will have gradual but progressive density-dependent and density-independent effects. For Scenario 3a, a harvest strategy with *h* = 0.01 corresponded to approximately $P_{t=35}^{N>MNPL}$ = 0.80 (Table 5). The starting harvest level for this strategy was 4 female bears/year. Scenario 3a demonstrates the potential for severe overexploitation when the capacity for growth is compromised. For example, a harvest strategy with *h* = 0.055 would result in near-certain subpopulation depletion (e.g., $P_{t=35}^{N>MNPL}$= 0.01), a high probability of crossing below the minimum abundance threshold ($P_{t=35}^{N>thresh}$ = 0.28), and a moderate probability of extirpation in the next 35 years (P_{ext} = 0.23). This is in strong contrast to Scenario 1, under which *h* = 0.055 was unlikely to have negative effects.

Population reconstruction for Scenario 3b used data and priors similar to Scenario 1, resulting in a similar estimate of r_{max} = 0.08. However, Scenario 3b included a nonlinear decline in *K* 1986-2016 that continued and accelerated during forward projections. Scenario 3b reflected the pessimistic hypothesis that, although the SH subpopulation will maintain its capacity for growth given sufficient habitat, loss of sea ice will result in a rapid and unidirectional collapse in *K* in the next 35 years. In contrast to Scenario 3a, subpopulation outcomes for Scenario 3b were insensitive to harvest (Table 6). A rapidly declining *K* guaranteed that *N* would decline as well. Furthermore, a high r_{max} allowed for a compensatory response to harvest. This meant that natural mortality due to declining *K* could be largely replaced by human-caused mortality, without accelerating subpopulation declines. Scenarios 3a and 3b are

extreme examples of density-independent and density-dependent effects of habitat loss, respectively. Furthermore, caution is required when interpreting results for Scenario 3b because it does not allow for the possibility that *K* will stabilize at a lower level or eventually recover, in which case harvest could contribute to extirpation that otherwise may have been avoidable. Although Scenarios 3a and 3b are both likely oversimplifications of how sea-ice loss might impact polar bears (e.g., Bromaghin et al. 2015), they demonstrate that the mechanisms of habitat change can have a strong influence on the effects of human-caused removals. These findings also provide a cautionary note for management because, without high quality scientific data, it will be difficult to distinguish between these scenarios.

We evaluated a wide range of harvest strategies, some of which may not be viable management options. For example, a harvest that is aggressive under Scenario 1 (e.g., $h = 0.06$) would have severe negative biological effects under all but optimal conditions. Conversely, a harvest that is conservative under Scenario 3a could result in lost opportunities for subsistence use. To evaluate the biological risks of harvest, we suggest orienting toward Scenario 2 at a moderate degree of risk tolerance with respect to Management Objective 1 in the near term. This approach would suggest female harvest rates of $h = 0.02$-0.03, which correspond to starting harvest levels of 8-12 female bears/year. This is equivalent to a total (i.e., female and male) harvest rate of approximately 2.0-3.0% assuming a 1:1 male-to-female sex ratio in the harvest, and a total harvest rate of approximately 3.0-4.5% assuming a 2:1 male-to-female sex ratio. These mid-range strategies have the benefit of limiting lost opportunities for use if conditions are more like Scenario 1, while reducing the chances of severe overexploitation if conditions are more like Scenario 3a. Working from this starting point, managers can weigh the pros and cons of lower and higher harvests in terms of biological risk, opportunities for use, and other considerations (e.g., human safety). Adherence to a 5-year management interval will facilitate adjustments to the harvest if new information suggests that management objectives are not being met.

Our assessment considered female bears only because the theta-logistic equation did not include a detailed model of reproduction. The benefits of sex-selective harvest have been demonstrated for multiple game species (e.g., White et al. 2001) and applied successfully to

polar bears (Obbard et al. 2010). Previous stochastic modeling has suggested that it is possible to harvest polar bears at a 2:1 male-to-female ratio without depleting males, provided that the female harvest remains below *MSY* (Taylor et al. 2008). We caution that Taylor et al. (2008) used values of *MSY* that are lower than some estimates from recent modeling, and that imperfect demographic information and time-lags in management can increase the chances of reducing adult males to the point where reproduction is compromised (Regehr et al. 2017b). The risk of overexploiting male bears could be mitigated, while still protecting females, by harvesting at a 2:1 sex ratio while using a conservative female harvest rate and monitoring subpopulation composition.

Management framework

Our analyses assume there will be a state-dependent harvest management framework in place for the SH subpopulation that can respond to future changes in subpopulation status. This requires a coupled research-management framework that can monitor the harvest, obtain periodic estimates of *N*, and use updated information to modify harvest levels. All simulations assumed that new aerial surveys will be completed every 5 years with a level of precision similar to the surveys in 2012 and 2016 (Obbard et al. 2015, 2018). Longer management intervals (i.e., > 5 years) would be associated with higher levels of risk for a given harvest strategy, because there would be fewer opportunities to identify and correct for overharvest resulting from biased estimates of demographic parameters, ecological change, or other factors. Similarly, lower precision in estimates of *N* would be associated with higher risk. If there is uncertainty in the ability to implement state-dependent harvest management with these conditions, adopting a more conservative approach to harvest will be necessary to mitigate risk. In future applications, it would be possible to evaluate the costs and benefits of research investment by modeling subpopulation assessments with different timing and levels of precision.

We evaluated harvest relative to three management objectives. Management Objective 1 sought to harvest at a level approaching maximum sustainable yield while implementing the

well-established safeguard of maintaining *N* > maximum net productivity level (*MNPL*; Regehr et al. 2017a, 2018a). Because *MNPL* is defined relative to a potentially changing *K*, this objective can accommodate changes in habitat (e.g., it does not seek to maintain an historic level of abundance in the face of habitat declines). In the current report, we focused on Management Objective 1 because it is well suited to balancing opportunities for use with protecting subpopulation viability when the environment is changing (USFWS 2016).

Management Objective 2 sought to maintain *N* above 90% of its starting value. We included this objective because similar metrics have been used in harvest risk assessments when habitat is stable and the goal is to prevent subpopulation declines (e.g., Taylor et al. 2006). Unlike Management Objective 1, this objective is defined relative to a static abundance and does not accommodate potential changes in *K*.

Management Objective 3 sought to maintain *N* above a minimum size at which the subpopulation would be demographically compromised. This objective does not provide a safeguard against overharvest and, if not used in conjunction with other biologically-sound management objectives, could lead to subpopulation depletion and the loss of opportunities for sustainable use. The number of bears corresponding to the minimum threshold likely varies across subpopulations as a function of multiple interacting factors. We subjectively used a threshold of 175 females because this value corresponds to a previously suggested value of 350 total bears (USFWS 2016), assuming that females comprise half of the SH subpopulation. We report Management Objective 3 because it conveys the probability that the subpopulation will become threatened to the extent that emergency management measures might be warranted. Threshold harvest rules, under which harvest is curtailed or closed below a pre-specified abundance level, can be an effective conservation measure (Fuller et al. 2015). USFWS (2016) expanded this concept to a three-level system under which graduated management and conservation actions are tied to pre-established thresholds (Figure 11). For example, if subpopulation abundance dropped below a certain level, it might trigger a research plan that included more frequent surveys or collection of detailed vital rates using capture-recapture methods. These thresholds and actions can extend beyond harvest to encompass a range of factors such as the type and intensity of monitoring, mitigation of human-bear conflicts, and

management of disturbance from industry and other human activities. Furthermore, the choice thresholds and actions can be made by the agencies responsible for research and management on a subpopulation basis. In light of uncertainties about the effects of climate change on the SH subpopulation, we suggest that a multi-level system of this type could help protect subpopulation viability while maintaining opportunities for use.

Demographic model

For long-lived species such as polar bears, population dynamics theory and empirical data (Fowler 1987, Wade 1998) suggest that most density-dependent change occurs at high population sizes (i.e., as *N* approaches *K*). The demographic model allowed for nonlinear density dependence by using a discrete version of the theta-logistic equation with a fixed value of the shape parameter θ (USFWS 2016). Because of its simple structure, the model has several limitations compared to more detailed models that are based on the polar bear life cycle and incorporate stage-specific vital rates (e.g., Regehr et al. 2017b). Specifically, the theta-logistic equation did not include sex structure, age structure, a mechanistic representation of reproduction or maternal care, the ability to consider individual differences in reproductive value or harvest vulnerability, positive density dependence (i.e., Allee effects), or differences in individual energetic requirements. Furthermore, we did not consider alternative values of the density-dependent shape parameter because data were too sparse to estimate θ specifically for the SH subpopulation (Clark et al. 2010). Johnson et al. (2018) suggested that the theta-logistic equation captured important population dynamics for an age-structured population of waterfowl, but comparative studies between the theta-logistic equation and matrix-based projection models have not been performed for polar bears. The structural limitations discussed above, together with uncertainties in the demographic data and other factors, mean that results from the demographic model should be interpreted with caution.

In the current report the effects of habitat loss are represented as density dependent (i.e., changing *K*), density independent (i.e., changing r_{max}), or both. The mechanisms of population change can influence the ability of a population to support harvest (Saether et al.

1996), as demonstrated by our simulations. For polar bears, both density-dependent and density-independent effects are possible (Regehr et al. 2017b) because sea-ice loss is both spatial and temporal in nature (Stern and Laidre 2016). Recent harvest risk assessments have assumed that the effects of habitat change are primarily density dependent, such that sea-ice loss leads to declines in K without concurrent changes in r_{max} (e.g., Regehr et al. 2018a). This assumption may be justified for subpopulations that are in the early stages of habitat loss and have a coupled research-management framework that can detect changes in N as well as density-independent changes in r_{max}. We evaluated both density-dependent and density-independent changes for the SH subpopulation because aerial surveys from the 2010s suggest that N may have already declined, and because current research does not provide information about vital rates, nutritional condition, or other factors that can help detect changes in r_{max}. Our simulations demonstrate how failure to reduce harvest rate in response to declines in r_{max} can lead to accelerated subpopulation declines.

We describe the demographic model in this report as provisional because it was developed under a timeline set by management needs and may not take advantage of all available biological information for the SH subpopulation. It does not propagate all sources of parametric, model-based, and environmental variation in an integrated manner and we did not perform sensitivity analyses to evaluate key assumptions, including the choice of prior distributions for parameters of the theta-logistic equation. Other potential areas for development include recasting the population reconstruction in a formal Bayesian framework, exploring mechanistic links between K and r_{max}, and investigating the potential for an integrated population model that could use all available data to directly estimate the demographic parameters needed for a harvest risk assessment.

Research and monitoring

Harvest risk assessments can help to identify data gaps and thus suggest future research, monitoring, and analytical approaches. Several biological questions in this report cannot be resolved with available data because current research on the SH subpopulation is

focused on the use of aerial surveys, which provide estimates of *N* but little additional biological or ecological information. The statistical power to detect changes in *N* from sequential aerial surveys can be low. Given evidence for declining abundance of the SH subpopulation during the period 2012-2016, and the implications for conservation and management if apparent declines continue or accelerate (e.g., similar to Scenarios 3a or 3b), priority should be placed on obtaining an updated abundance estimate from aerial surveys or other methods in the near future (e.g., ≤5 years). Application of satellite telemetry would provide data on polar bear movements and distribution (Obbard and Middel 2012) that can be critical for estimating unbiased demographic parameters. For example, Regehr et al. (2018b) developed an integrated population model for Chukchi Sea polar bears that concurrently analyzed capture-recapture and satellite telemetry data. Having data on animal movements made it possible to delineate temporary emigration from mortality (i.e., to determine whether animals left the study area or died), which was necessary to obtain estimates of survival and abundance that were useful for management (Regehr et al. 2018a). In general, physical capture-recapture studies provide information on population health, nutritional condition, movements, habitat use, and vital rates (Vongraven 2012) that can help improve our understanding of subpopulation status and frame the overall management approach. For example, information on range expansions and improved nutritional condition provided evidence that the Kane Basin subpopulation may be experiencing transient benefits from lighter sea-ice conditions (SWG 2016). Similarly, long-term declines in physical stature and condition (Stirling et al. 1999; Rode et al. 2010) have preceded evidence for demographic declines due to sea-ice loss in some other subpopulations (Regehr et al. 2007, 2010; Bromaghin et al. 2015; Lunn et al. 2016). In the context of managing human-caused removals, the information obtained from capture-recapture studies can allow a state-dependent approach under which both the harvest rate and harvest level can be adjusted in response to changing environmental conditions, resulting in a more robust system. In future applications, the demographic model could be used to assess the costs and benefits of alternative research methods (e.g., the extent to which having updated estimates of r_{max} could mitigate harvest risk).

Acknowledgements

Support for E. Regehr to perform analyses for the Provisional Harvest Risk Assessment for the Southern Hudson Bay Polar Bear Subpopulation was provided by Environment and Climate Change Canada and the University of Washington. Analytical advice and review were provided by M. Runge (U.S. Geological Survey). Sea-ice data were provided by H. Stern (University of Washington).

Supplementary Materials

Appendix 1: Example R-language function describing the demographic model for the SH polar bear subpopulation

Literature Cited

Atwood, T. C., B. G. Marcot, D. C. Douglas, S. C. Amstrup, K. D. Rode, G. M. Durner, and J. F. Bromaghin. 2016. Forecasting the relative influence of environmental and anthropogenic stressors on polar bears. Ecosphere 7: e01370, doi:10.1002/ecs2.1370.

Bromaghin, J. F., T. L. McDonald, I. Stirling, A. E. Derocher, E. S. Richardson, E. V. Regehr, D. C. Douglas, G. M. Durner, T. Atwood, and S. C. Amstrup. 2015. Polar bear population dynamics in the southern Beaufort Sea during a period of sea ice decline. Ecological Applications 25:634-651.

Clark, F., B. W. Brook, S. Delean, H. R. Akçakaya, and C. J. A. Bradshaw. 2010. The theta-logistic is unreliable for modelling most census data. Methods in Ecology and Evolution 1:253-262.

Derocher, A. E., N. J. Lunn, and I. Stirling. 2004. Polar bears in a warming climate. Integrative and Comparative Biology 44:163-176.

Devineau, O., R. Choquet, and J. D. Lebreton. 2006. Planning capture-recapture studies: straightforward precision, bias, and power calculations. Wildlife Society Bulletin 34:1028-1035.

Durner, G. M., K. L. Laidre, and G. S. York (eds). 2018. Polar Bears: Proceedings of the 18th Working Meeting of the IUCN/SSC Polar Bear Specialist Group, 7-11 June 2016, Anchorage, Alaska. IUCN, Gland, Switzerland and Cambridge, UK, xxx + 207pp.

Dyck, M. G. 2006. Characteristics of polar bears killed in defense of life and property in Nunavut, Canada, 1970-2000. Ursus 17:52-62.

Dyck, M., M. Campbell, D. Lee, J. Boulanger, and D. Hedman. 2017. 2016 Aerial Survey of the Western Hudson Bay Polar Bear Subpopulation. Final Report. Government of Nunavut, Department of Environment, Wildlife Research Section, Igloolik, Nunavut, Canada, 82 pp + 2 supplements.

Eberhardt, L. L. 1990. Survival rates required to sustain bear populations. Journal of Wildlife Management 54:587-590.

Fowler, C. W. 1987. A review of density dependence in populations of large mammals. Current Mammalogy 1:401-441.

Fuller, E., E. Brush, and M. L. Pinsky. 2015. The persistence of populations facing climate shifts and harvest. Ecosphere 6: 153, doi:10.1890/ES14-00533.1.

Houlahan, J. E., S. T. McKinney, T. M. Anderson, and B. J. McGill. 2017. The priority of prediction in ecological understanding. Oikos 126:1-7.

Gelman, A., and J. Hill. 2007. Data analysis using regression and multilevel/hierarchical models. Cambridge University Press, New York, New York, USA.

Guthery, F. S., and J. H. Shaw. 2013. Density dependence: Applications in wildlife management. Journal of Wildlife Management 77:33-38.

Johnson, F. A., M. Alhainen, A. D. Fox, J. Madsen, and M. Guillemain. 2018. Making do with less: must sparse data preclude informed harvest strategies for European waterbirds? Ecological Applications 28:427-441.

Kolenosky, G.B., K.F. Abraham, and C.J. Greenwood. 1992. Polar bears of southern Hudson Bay. Polar bear project, 1984-88. Final Report. Ontario Ministry of Natural Resources, Maple, Ontario, Canada, 107 pp.

Kolenosky, G. B., B. A. Pond, and K. F. Abraham. 1994. Population characteristics of polar bears in Southern Hudson Bay. International Conference on Bear Research and Management 9:301 (*abstract only)*.

Laforest, B. J., J. S. Hébert, M. E. Obbard, and G. W. Thiemann. 2018. Traditional Ecological Knowledge of polar bears in the northern Eeyou Marine Region, Québec, Canada. Arctic 71:40-58.

Laidre, K. L., H. Stern, K. M. Kovacs, L. Lowry, S. E. Moore, E. V. Regehr, S. H. Ferguson, Ø. Wiig, P. Boveng, R. P. Angliss, E. W. Born, D. Litovka, L. Quakenbush, C. Lydersen, D. Vongraven, and F. Ugarte. 2015. Arctic marine mammal population status, sea ice habitat loss, and conservation recommendations for the 21st century. Conservation Biology 29:724-737.

Lunn, N. J., S. Servanty, E. V. Regehr, S. J. Converse, E. Richardson, and I. Stirling. 2016. Demography of an apex predator at the edge of its range: impacts of changing sea ice on polar bears in Hudson Bay. Ecological Applications 26:1302-1320.

Lyons, J. E., M. C. Runge, H. P. Laskowski, and W. L. Kendall. 2008. Monitoring in the context of structured decision-making and adaptive management. Journal of Wildlife Management 72:1683-1692.

Mace, G. M., N. J. Collar, K. J. Gaston, C. Hilton-Taylor, H. R. Akçakaya, N. Leader-Williams, E. J. Milner-Gulland, and S. N. Stuart. 2008. Quantification of extinction risk: IUCN's system for classifying threatened species. Conservation Biology 22:1424-1442.

NMRWB [Nunavik Marine Regional Wildlife Board]. 2018. Nunavik Inuit Knowledge and Observations of Polar Bears: Polar Bears of the Southern Hudson Bay subpopulation. Project conducted and report prepared for the NMRWB by Basterfield, M., K. Breton-Honeyman, C. Furgal, J. Rae, and M. O'Connor. Inukjuak, Québec, Canada, xiv+73 pp.

Obbard, M. E., M. R. L. Cattet, E. J. Howe, K. R. Middel, E. J. Newton, G. B. Kolenosky, K. F. Abraham, and C. J. Greenwood. 2016. Trends in body condition in polar bears (*Ursus maritimus*) from the Southern Hudson Bay subpopulation in relation to changes in sea ice. Arctic Science 2:15-32.

Obbard, M. E., T. L. McDonald, E. J. Howe, E. V. Regehr, and E. S. Richardson. 2007. Polar Bear Population Status in Southern Hudson Bay, Canada. U.S. Geological Survey Administrative Report, Reston, Virginia, USA, 32 pp.

Obbard, M. E., and K. R. Middel. 2012. Bounding the Southern Hudson Bay polar bear population. Ursus 23:134-144.

Obbard, M. E., S. Stapleton, K. R. Middel, I. Thibault, V. Brodeur, and C. Jutras. 2015. Estimating the abundance of the Southern Hudson Bay polar bear subpopulation with aerial surveys. Polar Biology 38:1713-1725.

Obbard, M. E., S. Stapleton, G. Szor, K. R. Middel, C. Jutras, and M. Dyck. 2018. Re-assessing abundance of Southern Hudson Bay polar bears by aerial survey: effects of climate change at the southern edge of the range. Arctic Science 4:634-655.

Obbard, M. E., G. W. Thiemann, E. Peacock, and T. D. DeBruyn (eds). 2010. Polar Bears: Proceedings of the 15th Working Meeting of the IUCN/SSC Polar Bear Specialist Group, 29 June - 3 July 2009, Copenhagen, Denmark. IUCN, Gland, Switzerland and Cambridge, UK, vii + 235 pp.

Polar Bear Range States. 2015. Circumpolar Action Plan: Conservation Strategy for Polar Bears. A product of the representatives of the parties to the 1973 Agreement on the Conservation of Polar Bears, 80 pp. (available at <http://naalakkersuisut.gl/en/Naalakkersuisut/Departments/Fiskeri-Fangst-og-Landbrug/Isbjorn/The-Circumpolar-Action-Plan-and-Executive-Summary>).

Regehr, E. V., S. Atkinson, E. W. Born, K. L. Laidre, N. J. Lunn, and Ø. Wiig. 2017a. Harvest Assessment for the Baffin Bay and Kane Basin Polar Bear Subpopulations: Final Report to the Canada-Greenland Joint Commission on Polar Bear. 31 July 2017: iii + 107 pp.

Regehr, E. V., M. Ben-David, S. C. Amstrup, G. M. Durner, and J. S. Horne. 2009. Chapter 4. Quantifying bias in capture-recapture studies for mobile species: a case study with polar bears. In:Polar bear (*Ursus maritimus*) demography in relation to Arctic sea ice decline. PhD dissertation. University of Wyoming, Laramie, Wyoming, USA.

Regehr, E. V., N. J. Hostetter, R. R. Wilson, K. D. Rode, M. St. Martin, and S. J. Converse. 2018b. Integrated population modeling provides the first empirical estimates of vital rates and abundance for polar bears in the Chukchi Sea. Scientific Reports 8:16780, doi:10.1038/s41598-018-34824-7.

Regehr, E. V., C. M. Hunter, H. Caswell, S. C. Amstrup, and I. Stirling. 2010. Survival and breeding of polar bears in the southern Beaufort Sea in relation to sea ice. Journal of Animal Ecology 79:117-127.

Regehr, E. V., K. L. Laidre, H. R. Akçakaya, S. C. Amstrup, T. C. Atwood, N. J. Lunn, M. Obbard, H. Stern, G. W. Thiemann, and Ø. Wiig. 2016. Conservation status of polar bears (*Ursus maritimus*) in relation to projected sea-ice declines. Biology Letters 12:20160556, doi: 10.1098/rsbl.2016.0556.

Regehr, E. V., N. J. Lunn, S. C. Amstrup, and I. Stirling. 2007. Effects of earlier sea ice breakup on survival and population size of polar bears in western Hudson Bay. Journal of Wildlife Management 71:2673-2683.

Regehr, E. V., L. Polasek, A. Von Duyke, J. M. Wilder, and R. R. Wilson. 2018a. Harvest Risk Assessment for Polar Bears in the Chukchi Sea: Report to the Commissioners of the U.S.-Russia Polar Bear Agreement, 25 June 2018. Unpublished report, 95 pp.

Regehr, E. V., R. R. Wilson, K. D. Rode, and M. C. Runge. 2015. Resilience and Risk – a Demographic Model to Inform Conservation Planning for Polar Bears. U.S. Geological Survey Open-File Report 2015-1029, Reston, Virginia, USA, 56 pp.

Regehr, E. V., R. R. Wilson, K. D. Rode, M. C. Runge, and H. L. Stern. 2017b. Harvesting wildlife affected by climate change: a modeling and management approach for polar bears. Journal of Applied Ecology 54:1534-1543.

Rode, K. D., S. C. Amstrup, and E. V. Regehr. 2010. Reduced body size and cub recruitment in polar bears associated with sea ice decline. Ecological Applications 20:768-782.

Ross, J. V. 2009. A note on density dependence in population models. Ecological Modelling 220:3472-3474.

Saether, B.-E., S. Engen, and R. Lande. 1996. Density-dependence and optimal harvesting of fluctuating populations. Oikos 76:40-46.

Saether, B.-E., S. Engen, and E. Matthysen. 2002. Demographic characteristics and population dynamical patterns of solitary birds. Science 295:2070-2073.

Sciullo, L., G. W. Thiemann, and N. J. Lunn. 2016. Comparative assessment of metrics for monitoring the body condition of polar bears in western Hudson Bay. Journal of Zoology 300:45-58.

Shadbolt, T., G. York, and E. W. T. Cooper. 2012. Icon on Ice: International Trade and Management of Polar Bears. TRAFFIC North America and WWF-Canada, Vancouver, British Columbia, Canada, vii + 169 pp.

Stapleton, S., S. Atkinson, D. Hedman, and D. Garshelis. 2014. Revisiting Western Hudson Bay: Using aerial surveys to update polar bear abundance in a sentinel population. Biological Conservation 170:38-47.

Stern, H. L., and K. L. Laidre. 2016. Sea-ice indicators of polar bear habitat. The Cryosphere 10:2027-2041.

Stirling, I., N. J. Lunn, and J. Iacozza. 1999. Long-term trends in the population ecology of polar bears in Western Hudson Bay in relation to climatic change. Arctic 52:294-306.

Stott, I., S. Townley, and D. J. Hodgson. 2011. A framework for studying transient dynamics of population projection matrix models. Ecology Letters 14:959-970.

Stubben, C., and B. Milligan. 2007. Estimating and analyzing demographic models using the popbio package in R. Journal of Statistical Software 22:1-23.

Sutherland, W. J. 2001. Sustainable exploitation: a review of principles and methods. Wildlife Biology 7:131-140.

SWG [Scientific Working Group to the Canada-Greenland Joint Commission on Polar Bear]. 2016. Re-Assessment of the Baffin Bay and Kane Basin Polar Bear Subpopulations: Final Report to the Canada-Greenland Joint Commission on Polar Bear. 31 July 2016: x + 636 pp.

Taylor, M. K., D. P. DeMaster, F. L. Bunnell, and R. E. Schweinsburg. 1987. Modeling the sustainable harvest of female polar bears. Journal of Wildlife Management 51:811-820.

Taylor, M. K., J. Laake, P. D. McLoughlin, H. D. Cluff, and F. Messier. 2006. Demographic parameters and harvest-explicit population viability analysis for polar bears in M'Clintock Channel, Nunavut, Canada. Journal of Wildlife Management 70:1667-1673.

Taylor, M. K., P. D. McLoughlin, and F. Messier. 2008. Sex-selective harvesting of polar bears *Ursus maritimus*. Wildlife Biology 14:52-60.

Taylor, M., M. Obbard, B. Pond, M. Kuc, and D. Abraham. 2006. A Guide to Using RISKMAN: Stochastic and Deterministic Population Modeling RISK MANagement Decision Tool for Harvested and Unharvested Populations. The Queen's Printer for Ontario, Toronto, Ontario, Canada, 58 pp.

USFWS [U.S. Fish and Wildlife Service]. 2016. Polar Bear (*Ursus maritimus*) Conservation Management Plan, Final. U.S. Fish and Wildlife Service, Region 7, Anchorage, Alaska, USA, 59 pp.

Viengkone, M., A. E. Derocher, E. S. Richardson, M. E. Obbard, M. G. Dyck, N. J. Lunn, V. Sahanatien, B. G. Robinson, and C. S. Davis. 2018. Assessing spatial discreteness of Hudson Bay polar bear populations using telemetry and genetics. Ecosphere 9:e02364, doi:10.1002/ecs2.2364.

Vongraven, D., J. Aars, S. Amstrup, S. N. Atkinson, S. Belikov, E. W. Born, T. D. DeBruyn, A. E. Derocher, G. Durner, M. Gill, N. Lunn, M. E. Obbard, J. Omelak, N. Ovsyanikov, E. Peacock, E. Richardson, V. Sahanatien, I. Stirling, and Ø. Wiig. 2012. A circumpolar monitoring framework for polar bears. Ursus Monograph Series 5:1-66.

Wade, P. R. 1998. Calculating limits to the allowable human-caused mortality of cetaceans and pinnipeds. Marine Mammal Science 14:1-37.

White, G. C., D. J. Freddy, R. B. Gill, and J. H. Ellenberger. 2001. Effect of adult sex ratio on mule deer and elk productivity in Colorado. Journal of Wildlife Management 65:543-551.

Wilder, J. M., D. Vongraven, T. Atwood, B. Hansen, A. Jessen, A. Kochnev, G. York, R. Vallender, D. Hedman, and M. Gibbons. 2017. Polar bear attacks on humans: implications of a changing climate. Wildlife Society Bulletin 41:537-547.

Williams, B. K., J. D. Nichols, and M. J. Conroy. 2002. Analysis and Management of Animal Populations. Academic Press, San Diego, California, USA, 817 pp.

Williams, C. K. 2013. Accounting for wildlife life-history strategies when modeling stochastic density-dependent populations: A review. Journal of Wildlife Management 77:4-11.

Winship, A. J., and A. W. Trites. 2006. Risk of extirpation of Steller sea lions in the Gulf of Alaska and Aleutian Islands: A population viability analysis based on alternative hypotheses for why sea lions declined in western Alaska. Marine Mammal Science 22:124-155.

Tables and Figures

Table 1. Abbreviations, parameters, and indexing definitions used in the demographic model for the Southern Hudson Bay polar bear subpopulation.

Term	Definition
CV	Coefficient of variation, defined as a ratio of the standard deviation to the mean of a statistical distribution of values. The CV reflects the level of uncertainty in an estimate, compared to the value of the estimate.
h	Harvest rate, defined as the percentage of subpopulation abundance that is removed each year through harvest. Unless otherwise noted, *h* refers to the female harvest rate, which is the proportion of females removed annually.
h^{total*}	Total (i.e. female and male) harvest rate expressed as the proportion of total bears removed annually assuming a 2:1 male-to-female ratio in removals.
H	Harvest level, measured in numbers of female polar bears removed each year.
$\bar{H}_t$	Mean annual female harvest level at timestep *t* during subpopulation projections.
κ	A dimensionless metric representing proportional changes in carrying capacity (*K*), calculated from the number of ice-covered days per year
K	Environmental carrying capacity, defined as the maximum number of individuals in a subpopulation that can be supported by the environment. In this report, *K* is measured in numbers of female polar bears and does not consider age structure or other factors.
$\bar{K}_t$	Mean carrying capacity at timestep *t* during subpopulation projections.
management interval	The number of years between successive subpopulation studies and changes to the calculated harvest level based on updated estimates of abundance and vital rates.
MNPL	The subpopulation abundance that results in the greatest net annual increment in subpopulation numbers resulting from reproduction minus losses due to natural mortality. The value of *MNPL* depends on how density dependence operates in a subpopulation.
MSY	Maximum sustainable yield.

N	Subpopulation abundance, measured in numbers of female polar bears unless otherwise noted. Subpopulation abundance in the demographic model does not reflect age or reproductive structure.
$\widetilde{N}$	An estimate of subpopulation abundance selected as the 50th percentile of its sampling distribution, used to calculate harvest level under a state-dependent harvest management approach.
$\bar{N}_t$	Mean subpopulation abundance at timestep t during subpopulation projections.
P_{ext}	Probability of extirpation, defined as abundance falling below a quasi-extinction threshold of 15% of starting subpopulation size.
$P_t^{N>MNPL}$	Probability that abundance is greater than maximum net productivity level (*MNPL*) at annual timestep t. This metric is used for Management Objective 1.
$P_t^{N>0.9N1}$	Probability that abundance is above 90% of starting abundance at annual timestep t. This metric is used for Management Objective 2.
$P_t^{N>threshold}$	Probability that abundance is above a minimum threshold of 175 female bears at annual timestep t. This metric is used for Management Objective 3.
PBSG	Polar Bear Specialist Group of the International Union for the Conservation of Nature.
r_{max}, r_{pot}, r_{MNPL}	Intrinsic population growth rates. The maximum intrinsic growth rate (r_{max}) occurs at a low density relative to carrying capacity; r_{pot} is a potential growth rate at an unspecified density; r_{MNPL} refers is the potential growth rate at a density referenced to maximum net productivity level. Values of r refer to unharvested, potential growth rates that provide measures of the resilience of a subpopulation.
risk tolerance	A statement of the required probability of meeting a management objective. Low risk tolerance generally implies a conservative approach that is very likely to meet objectives, while high risk tolerance implies a less conservative approach that accepts more risk of not meeting objectives.
S	Unharvested survival rate.
S^{total}	Total survival rate, which includes harvest mortality.
sd	Standard deviation, a statistical measure that quantifies the amount of variation of a set of numbers around the mean (i.e., average) value.

se	Standard error, a statistical measure that quantifies the amount of variation associated with an estimated parameter
SH subpopulation	The Southern Hudson Bay subpopulation of polar bears as recognized by the Polar Bear Specialist Group (PSBG) of the International Union for the Conservation of Nature. In the report we follow the example of the PBSG by referring to polar bear "subpopulations", except when using common terminology (e.g., "population projections").
state-dependent harvest management	An approach to harvest management under which harvest depends on the current status (i.e., "state") of a subpopulation. Under state-dependent harvest management, harvest levels are updated periodically (e.g., every 10 years) based on new estimates of abundance and vital rates obtained from scientific studies.
t	Year. When used to reference annual time steps during subpopulation projections, t = 1, 2, …, T.
θ	A parameter in the theta-logistic equation that determines the relationship between population density and population growth.

Table 2. Estimates of total (i.e., female and male) abundance for the Southern Hudson Bay polar bear subpopulation used to inform development of a provisional demographic model. Methods to derive these values are explained in the main text.

Year	Total abundance (95% CI)	Proportion female
1986	802 (564-1044)	0.46
1986*	733 (496-975)	0.46
2005	842 (564-1118)	0.57
2005*	773 (496-1050)	0.57
2012	943 (650-1312)	0.50
2016	781 (590-1023)	0.50

*Estimates of abundance for 1986 and 2005 that have not been adjusted for bears on the small islands in James Bay and islands in eastern Hudson Bay.

Table 3. Subpopulation outcomes for simulations under Scenario 1, the most optimistic scenario for the Southern Hudson Bay polar bear subpopulation. $\overline{H}_t$ is the harvest level (female bears/year) at time step t; *h* is the time-constant female harvest rate expressed as the proportion of female bears removed annually; h^{total*} is the time-constant total (i.e. female and male) harvest rate expressed as the proportion of total bears removed annually assuming a 2:1 male-to-female ratio in removals; $\overline{N}_{t=35}$ is mean female abundance; $\overline{K}_{t=35}$ is mean environmental carrying capacity; and P_{ext} is the probability of extirpation. $P_{t=35}^{N>MNPL}$, $P_{t=35}^{N>0.9N1}$, and $P_{t=35}^{N>thresh}$ are the probabilities of meeting management objectives 1, 2, and 3, respectively. Management objectives are defined in the main text. Most outcomes are referenced to the final time step *t* = 35.

$\overline{H}_{t=1}$	*h*	h^{total*}	$\overline{N}_{t=35}$	$\overline{K}_{t=35}$	$\overline{H}_{t=35}$	P_{ext}	$P_{t=35}^{N>MNPL}$	$P_{t=35}^{N>0.9N1}$	$P_{t=35}^{N>thresh}$
0	0.000	0.000	424	437	0	0.00	0.99	0.97	1.00
2	0.005	0.008	421	437	2	0.00	0.99	0.97	1.00
4	0.010	0.015	418	437	4	0.00	0.99	0.97	1.00
6	0.015	0.023	414	437	6	0.00	0.99	0.97	1.00
8	0.020	0.030	410	437	8	0.00	0.99	0.97	1.00
10	0.025	0.038	404	437	10	0.00	0.99	0.97	1.00
12	0.030	0.045	398	437	12	0.00	0.99	0.95	1.00
14	0.035	0.053	391	437	14	0.00	0.98	0.92	1.00
16	0.040	0.060	382	437	16	0.00	0.97	0.85	1.00
18	0.045	0.068	372	437	17	0.00	0.94	0.76	1.00
20	0.050	0.075	359	437	18	0.00	0.87	0.63	1.00
21	0.055	0.083	343	437	19	0.00	0.78	0.50	0.99
23	0.060	0.090	324	437	20	0.00	0.67	0.36	0.97

Table 4. Subpopulation outcomes for simulations under Scenario 2, a middle-of-the-road scenario for the Southern Hudson Bay polar bear subpopulation. $\overline{H}_t$ is the harvest level (female bears/year) at time step t; *h* is the time-constant female harvest rate expressed as the proportion of female bears removed annually; h^{total*} is the time-constant total (i.e. female and male) harvest rate expressed as the proportion of total bears removed annually assuming a 2:1 male-to-female ratio in removals; $\overline{N}_{t=35}$ is mean female abundance; $\overline{K}_{t=35}$ is mean environmental carrying capacity; and P_{ext} is the probability of extirpation. $P_{t=35}^{N>MNPL}$, $P_{t=35}^{N>0.9N1}$, and $P_{t=35}^{N>thresh}$ are the probabilities of meeting management objectives 1, 2, and 3, respectively. Management objectives are defined in the main text. Most outcomes are referenced to the final time step *t* = 35.

$\overline{H}_{t=1}$	*h*	h^{total*}	$\overline{N}_{t=35}$	$\overline{K}_{t=35}$	$\overline{H}_{t=35}$	P_{ext}	$P_{t=35}^{N>MNPL}$	$P_{t=35}^{N>0.9N1}$	$P_{t=35}^{N>thresh}$
0	0.000	0.000	466	474	0	0.00	1.00	1.00	1.00
2	0.005	0.008	456	474	2	0.00	0.99	0.99	1.00
4	0.010	0.015	443	474	4	0.00	0.99	0.98	1.00
6	0.015	0.023	429	474	7	0.00	0.97	0.96	1.00
8	0.020	0.030	412	474	8	0.00	0.92	0.89	1.00
10	0.025	0.038	392	474	10	0.00	0.84	0.81	0.99
12	0.030	0.045	369	474	11	0.00	0.75	0.70	0.98
14	0.035	0.053	344	474	12	0.00	0.63	0.57	0.96
16	0.040	0.060	316	474	13	0.00	0.51	0.43	0.90
18	0.045	0.068	286	474	13	0.00	0.38	0.29	0.83
20	0.050	0.075	255	474	13	0.00	0.26	0.19	0.74
21	0.055	0.083	222	474	13	0.02	0.17	0.11	0.64
23	0.060	0.090	190	474	12	0.06	0.10	0.06	0.52

Table 5. Subpopulation outcomes for simulations under Scenario 3a, a pessimistic scenario with strong density-independent limitation for the Southern Hudson Bay polar bear subpopulation. $\overline{H}_t$ is the harvest level (female bears/year) at time step t; *h* is the time-constant female harvest rate expressed as the proportion of female bears removed annually; h^{total*} is the time-constant total (i.e. female and male) harvest rate expressed as the proportion of total bears removed annually assuming a 2:1 male-to-female ratio in removals; $\overline{N}_{t=35}$ is mean female abundance; $\overline{K}_{t=35}$ is mean environmental carrying capacity; and P_{ext} is the probability of extirpation. $P_{t=35}^{N>MNPL}$, $P_{t=35}^{N>0.9N1}$, and $P_{t=35}^{N>thresh}$ are the probabilities of meeting management objectives 1, 2, and 3, respectively. Management objectives are defined in the main text. Most outcomes are referenced to the final time step *t* = 35.

$\overline{H}_{t=1}$	*h*	h^{total*}	$\overline{N}_{t=35}$	$\overline{K}_{t=35}$	$\overline{H}_{t=35}$	P_{ext}	$P_{t=35}^{N>MNPL}$	$P_{t=35}^{N>0.9N1}$	$P_{t=35}^{N>thresh}$
0	0.000	0.000	492	518	0	0.00	0.99	1.00	1.00
2	0.005	0.008	463	518	2	0.00	0.91	0.95	1.00
4	0.010	0.015	432	518	4	0.00	0.79	0.81	1.00
6	0.015	0.023	400	518	6	0.00	0.67	0.70	1.00
8	0.020	0.030	367	518	8	0.00	0.56	0.59	0.98
10	0.025	0.038	332	518	9	0.00	0.46	0.48	0.90
12	0.030	0.045	297	518	9	0.00	0.36	0.39	0.80
14	0.035	0.053	262	518	10	0.00	0.25	0.29	0.69
16	0.040	0.060	227	518	10	0.00	0.15	0.18	0.58
18	0.045	0.068	192	518	9	0.01	0.07	0.08	0.48
20	0.050	0.075	156	518	8	0.10	0.02	0.02	0.38
21	0.055	0.083	122	518	7	0.23	0.01	0.00	0.28
23	0.060	0.090	92	518	6	0.35	0.00	0.00	0.19

Table 6. Subpopulation outcomes for simulations under Scenario 3b, a pessimistic scenario with strong density-dependent regulation for the Southern Hudson Bay polar bear subpopulation. $\overline{H}_t$ is the harvest level (female bears/year) at time step t; *h* is the time-constant female harvest rate expressed as the proportion of female bears removed annually; h^{total*} is the time-constant total (i.e. female and male) harvest rate expressed as the proportion of total bears removed annually assuming a 2:1 male-to-female ratio in removals; $\overline{N}_{t=35}$ is mean female abundance; $\overline{K}_{t=35}$ is mean environmental carrying capacity; and P_{ext} is the probability of extirpation. $P_{t=35}^{N>MNPL}$, $P_{t=35}^{N>0.9N1}$, and $P_{t=35}^{N>thresh}$ are the probabilities of meeting management objectives 1, 2, and 3, respectively. Management objectives are defined in the main text. Most outcomes are referenced to the final time step *t* = 35.

$\overline{H}_{t=1}$	*h*	h^{total*}	$\overline{N}_{t=35}$	$\overline{K}_{t=35}$	$\overline{H}_{t=35}$	P_{ext}	$P_{t=35}^{N>MNPL}$	$P_{t=35}^{N>0.9N1}$	$P_{t=35}^{N>thresh}$
0	0.000	0.000	107	126	0	0.56	0.41	0.09	0.30
2	0.005	0.008	107	126	1	0.56	0.41	0.09	0.30
4	0.010	0.015	107	126	1	0.56	0.42	0.09	0.30
6	0.015	0.023	108	126	2	0.55	0.42	0.09	0.30
8	0.020	0.030	107	126	3	0.55	0.42	0.08	0.30
10	0.025	0.038	107	126	3	0.55	0.43	0.08	0.30
12	0.030	0.045	107	126	4	0.54	0.43	0.08	0.30
14	0.035	0.053	106	126	4	0.54	0.43	0.07	0.30
16	0.040	0.060	105	126	5	0.54	0.44	0.06	0.30
18	0.045	0.068	104	126	5	0.53	0.44	0.04	0.30
20	0.050	0.075	102	126	6	0.53	0.43	0.03	0.29
21	0.055	0.083	100	126	6	0.53	0.42	0.02	0.28
23	0.060	0.090	96	126	7	0.52	0.41	0.01	0.27

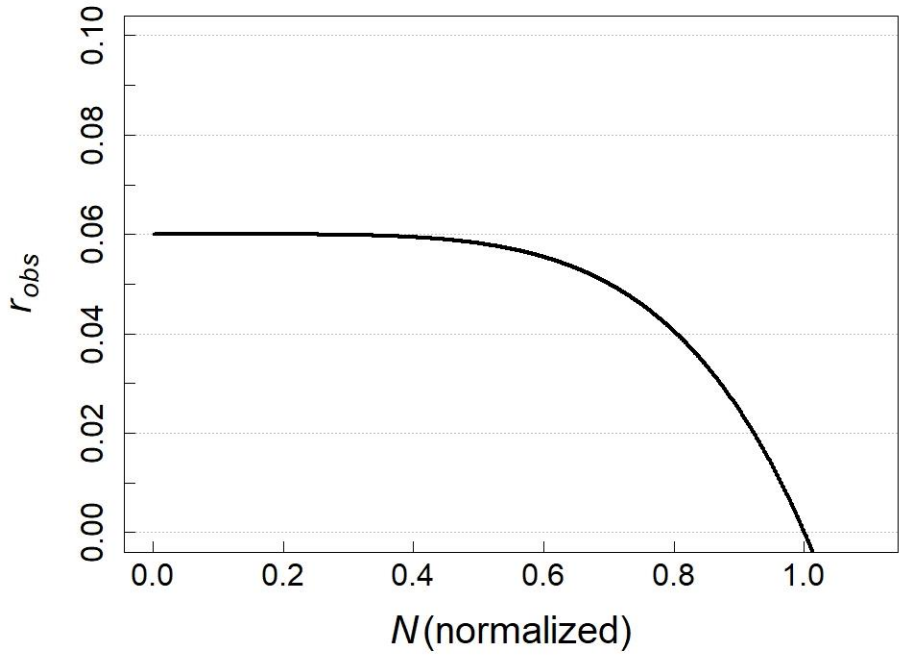

Figure 1. Example growth curve derived from a theta-logistic equation with the density-dependent shape parameter θ = 5.045 and maximum intrinsic growth rate r_{max} = 0.06. The x-axis is normalized abundance (N) such that environmental carrying capacity (K) occurs at N = 1. The y-axis is the observed growth rate (r_{obs}), which is equivalent to r_{max} at low densities and declines rapidly to 0 as $N/K \rightarrow 1$.

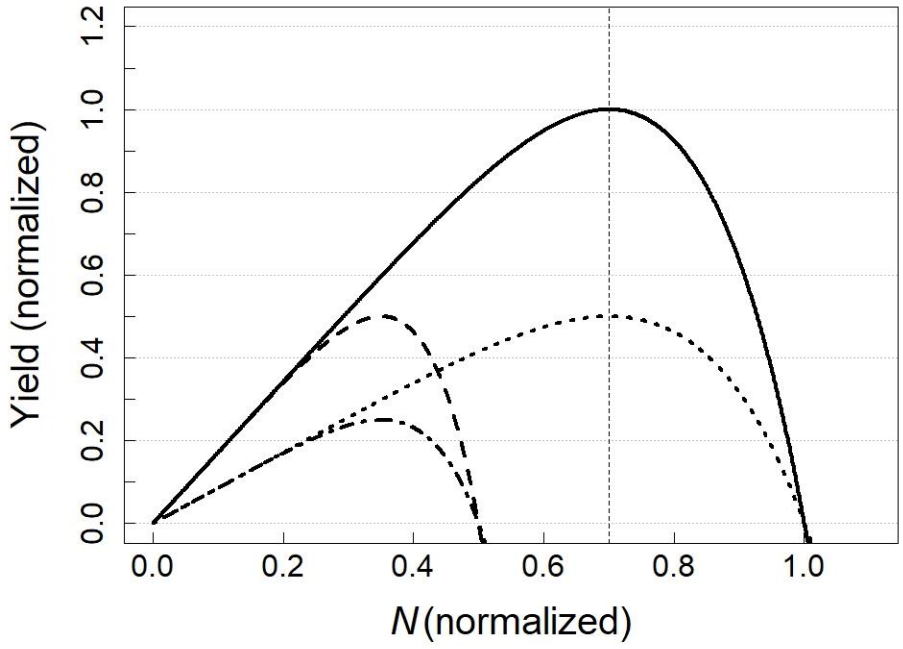

Figure 2. Example yield curves derived from a theta-logistic equation with the density-dependent shape parameter θ = 5.045. The solid black line is an example baseline curve with environmental carrying capacity K = 1 and maximum intrinsic growth rate r_{max} = 0.06. The x-axis is normalized abundance (N) such that environmental carrying capacity (K) occurs at N = 1 for the baseline curve. The y-axis is normalized yield such that maximum sustainable yield MSY = 1 for the baseline curve. The vertical dashed line represents maximum net productivity level, the subpopulation abundance at which maximum sustainable yield is achieved for the baseline curve. The dotted line shows the yield curve that would result if r_{max} was reduced to 0.03. The dashed line shows the yield curve if K was reduced to 0.5. The dot-dash line shows the yield curve if both r_{max} and K were reduced. The current demographic model does not include a mechanistic link between r_{max} and K.

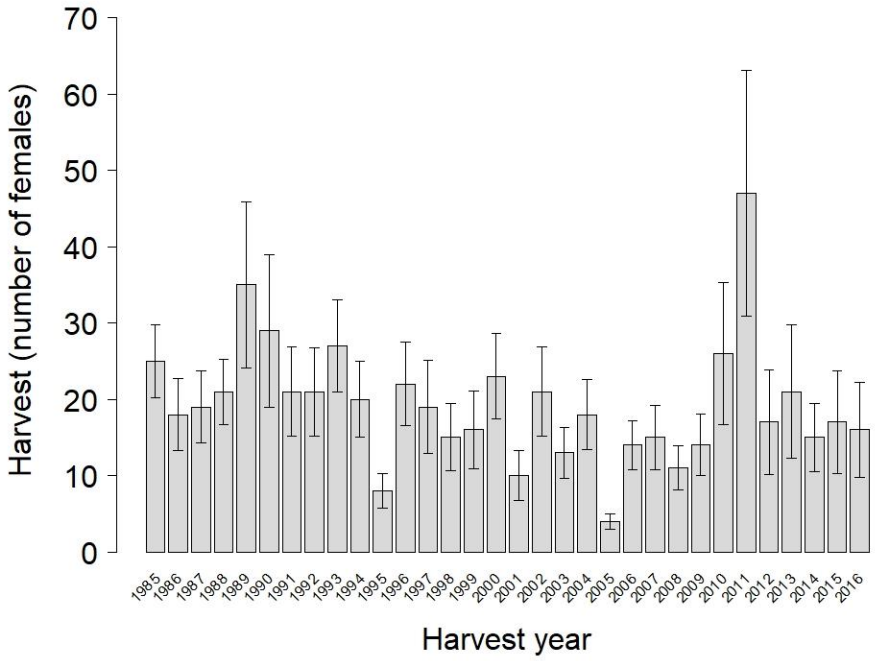

Figure 3. Approximate numbers of female polar bears removed by humans per harvest year in the Southern Hudson Bay polar bear subpopulation. Uncertainty in annual harvest numbers is represented by 95% confidence intervals (black error bars).

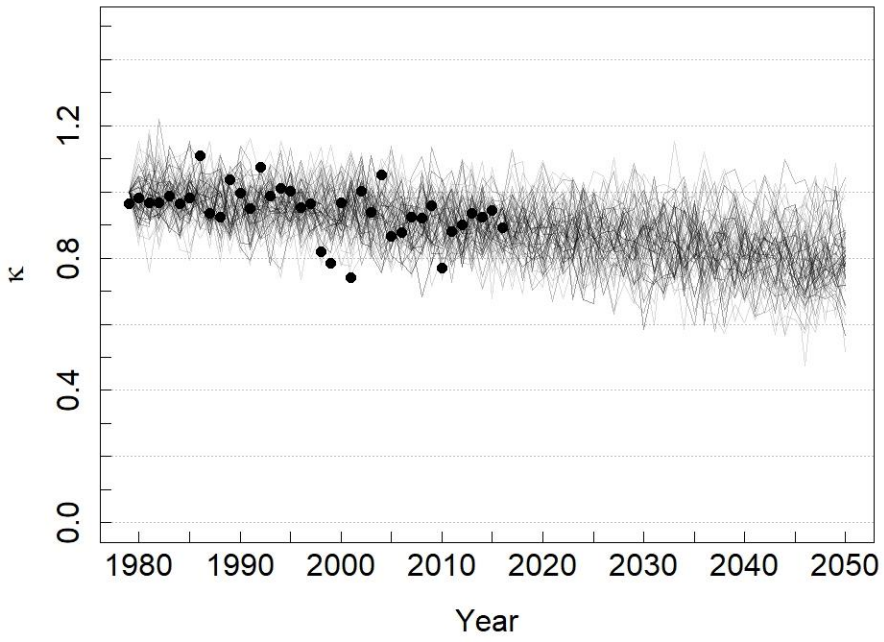

Figure 4. Stochastic projections (black lines) of the dimensionless parameter κ, which can be used in the demographic model to represent changes in environmental carrying capacity. The parameter κ was derived by standardizing the number of ice-covered days per year in the Southern Hudson Bay subpopulation boundary, as explained in the main text. Black dots represent standardized values of the observed number of ice-free days since the start of the satellite record. In this example, κ is projected forward for 35 years (approximately three polar bear generations) based on the slope of a linear model fit to the 1979-2016 sea-ice data.

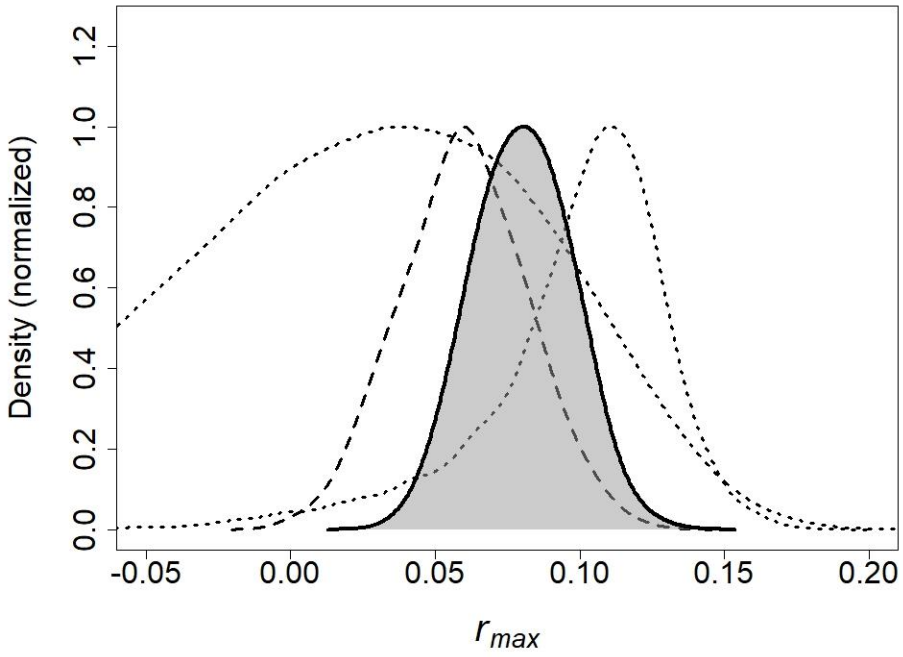

Figure 5. Distributions of maximum intrinsic growth rate (r_{max}) for the southern Hudson Bay polar bear subpopulation. The solid line with gray shading is the posterior distribution of r_{max} that was estimated using population reconstruction for Scenario 1. The dashed line is the prior for r_{max} derived from other case studies for polar bears. The two dotted lines are empirical estimates of r_{max} for 1986 (right curve) and 2005 (left curve) based on vital rates estimated from capture-recapture studies.

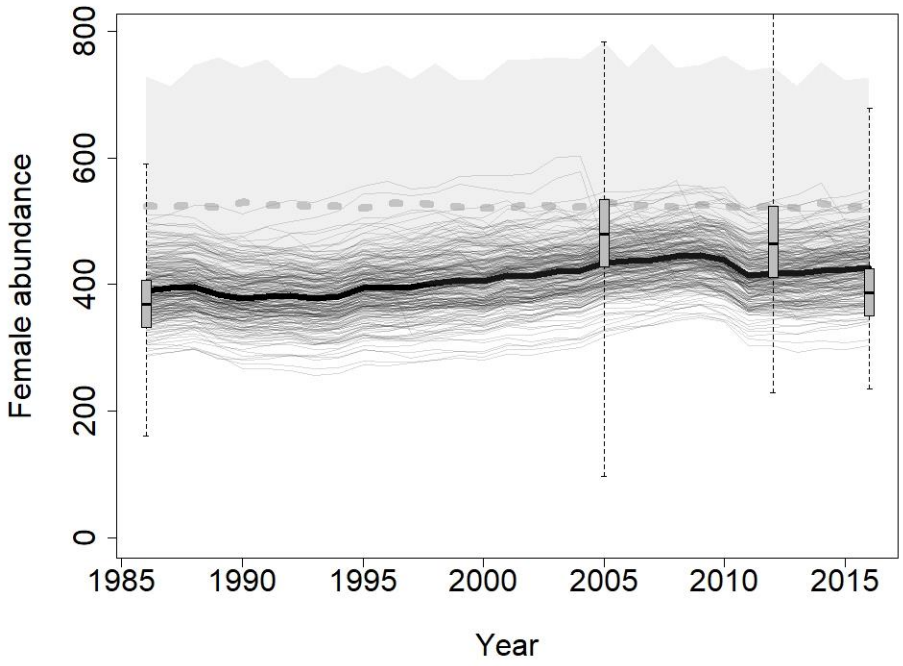

Figure 6. Scenario 1 population reconstruction: a sample of retrospective projections for female polar bears in the Southern Hudson Bay subpopulation, 1986-2016, using the theta-logistic model. The thin black lines are individual stochastic projections. The thick black line is the mean value of projected subpopulation abundance. In the background, the dashed light-gray line is the mean environmental carrying capacity (*K*) and the light-gray polygon represents the 95% confidence intervals on *K*. The box plots show the median, first and third quartiles, and range of empirical estimates of female abundance from capture-recapture studies (Obbard et al. 2007) and aerial surveys (Obbard et al. 2015, 2018).

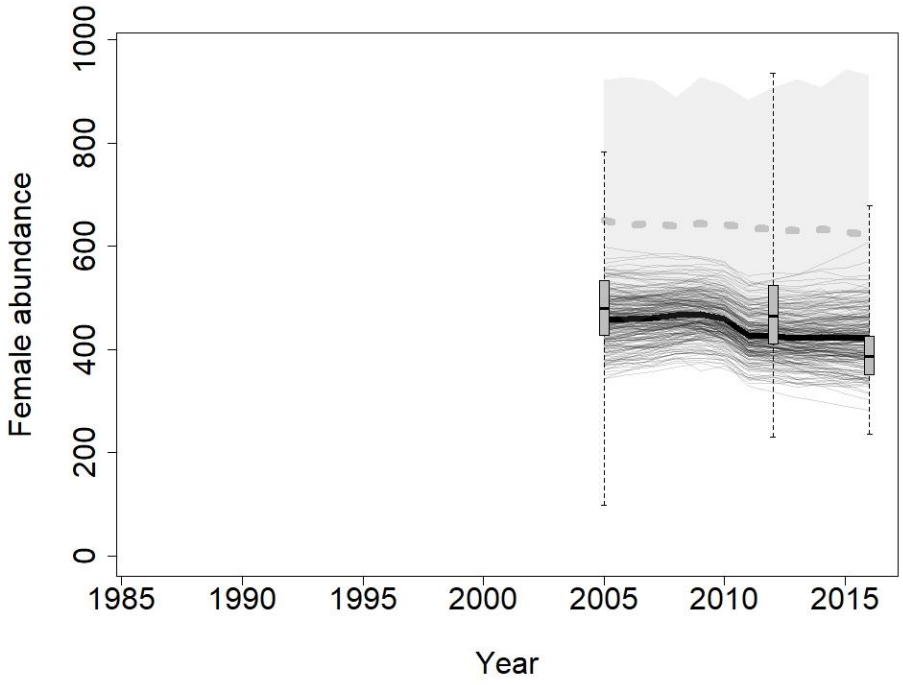

Figure 7. Scenario 2 population reconstruction: a sample of retrospective projections for female polar bears in the Southern Hudson Bay subpopulation, 2005-2016, using the theta-logistic model. The thin black lines are individual stochastic projections. The thick black line is the mean value of projected subpopulation abundance. In the background, the dashed light-gray line is the mean environmental carrying capacity (*K*) and the light-gray polygon represents the 95% confidence intervals on *K*. The box plots show the median, first and third quartiles, and range of empirical estimates of female abundance from capture-recapture studies (Obbard et al. 2007) and aerial surveys (Obbard et al. 2015, 2018).

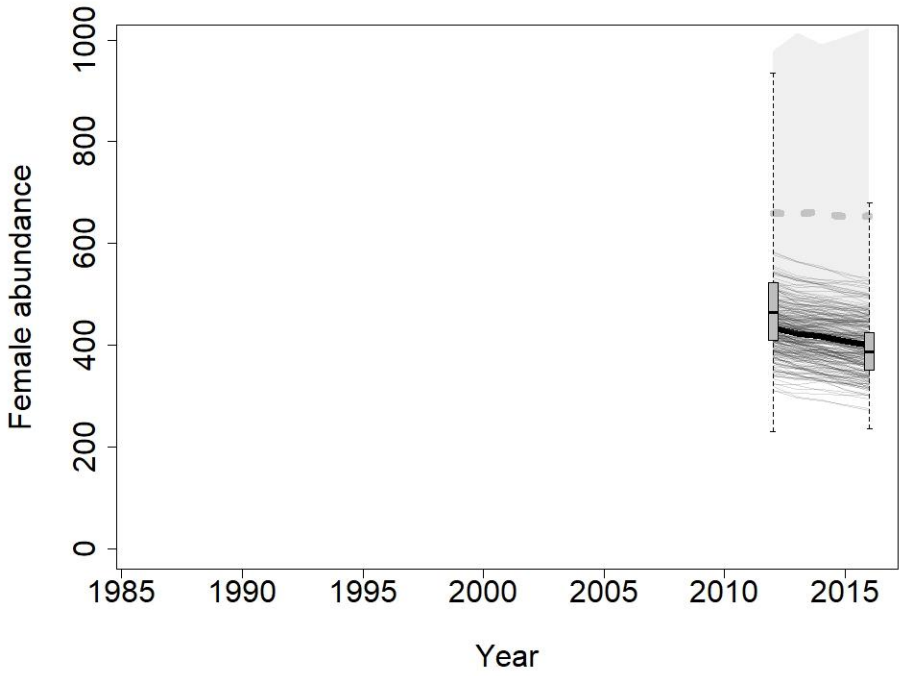

Figure 8. Scenario 3a population reconstruction: a sample of retrospective projections for female polar bears in the Southern Hudson Bay subpopulation, 2012-2016, using the theta-logistic model. The thin black lines are individual stochastic projections. The thick black line is the mean value of projected subpopulation abundance. In the background, the dashed light-gray line is the mean environmental carrying capacity (*K*) and the light-gray polygon represents the 95% confidence intervals on *K*. The box plots show the median, first and third quartiles, and range of empirical estimates of female abundance from aerial surveys (Obbard et al. 2015, 2018).

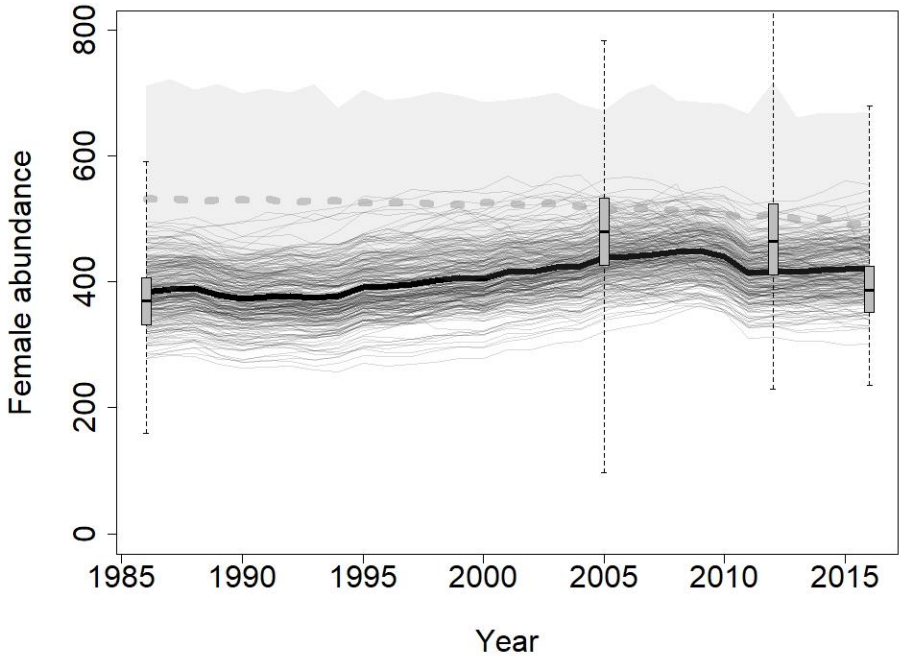

Figure 9. Scenario 3b population reconstruction: a sample of retrospective projections for female polar bears in the Southern Hudson Bay subpopulation, 1986-2016, using the theta-logistic model. The thin black lines are individual stochastic projections. The thick black line is the mean value of projected subpopulation abundance. In the background, the dashed light-gray line is the mean environmental carrying capacity (*K*) and the light-gray polygon represents the 95% confidence intervals on *K*. The box plots show the median, first and third quartiles, and range of empirical estimates of female abundance from capture-recapture studies (Obbard et al. 2007) and aerial surveys (Obbard et al. 2015, 2018).

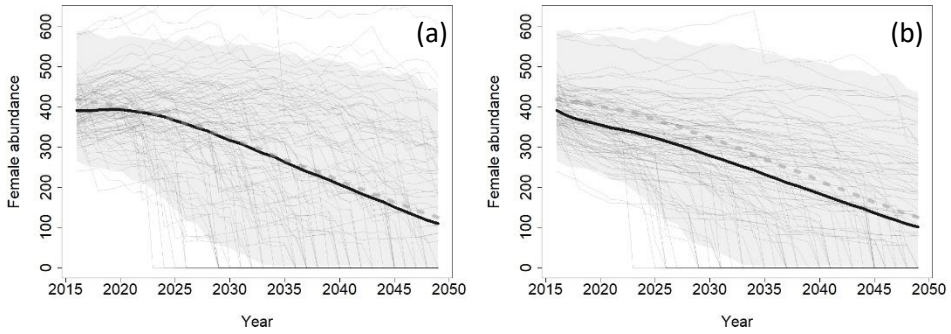

Figure 10. Scenario 3b forward projections: a sample of retrospective projections for female polar bears in the Southern Hudson Bay subpopulation, 2016-2049, using the theta-logistic model. The thin black lines are individual stochastic projections. The thick black line is the mean value of projected subpopulation abundance. In the background, the dashed light-gray line is the mean environmental carrying capacity (*K*) and the light-gray polygon represents the 95% confidence intervals on *K*. Panel (a) represents projections with a female harvest rate *h* = 0.00. Panel (b) represents projections with a female harvest rate *h* = 0.055, which corresponds to a starting harvest level of approximately 21 bears/year.

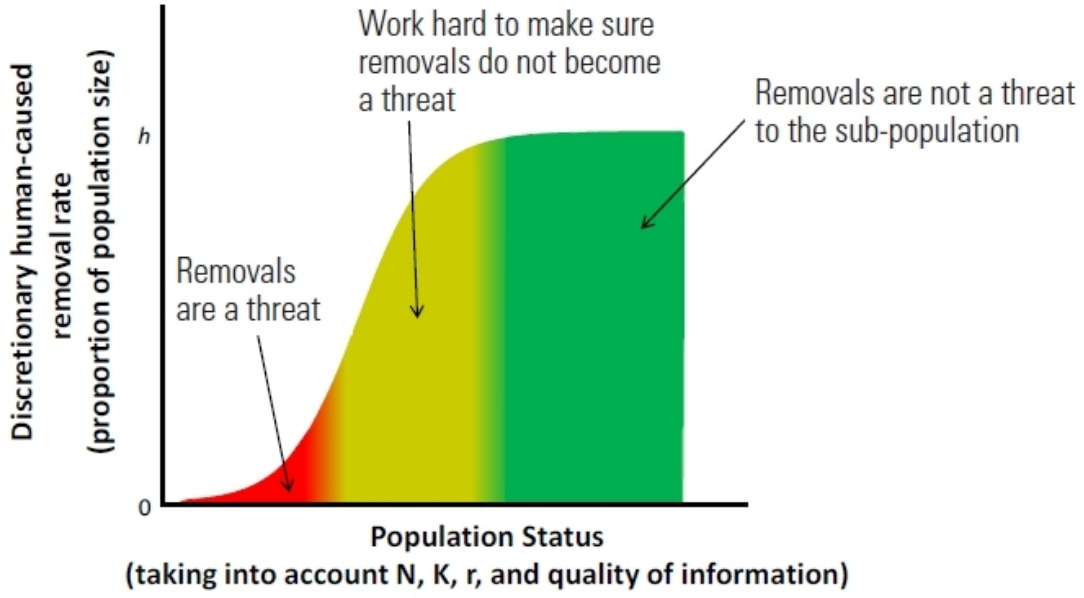

Figure 11 (reproduced with permission from USFWS 2016, Figure 8). Three-level framework for management of polar bear take. In the green zone, the maximum number of annual removals is proportional to the population size, with the proportion (the rate) sensitive to any changes in the intrinsic rate of growth of the population. In the yellow zone, additional efforts are warranted, including consideration of increased monitoring effort, reduction of defense-of-life or other removals, and reduction in subsistence harvest. In the red zone, emergency measures to reduce or minimize all human-caused removals are recommended. In all three zones, the colored region represents the range of removal rates that meet the conservation guidelines of this Plan [USFWS 2016]; the local choice of where to fall within those bounds can take into account the specific context of the subpopulation.

Appendix 1: Example R-language function describing the demographic model for the SH polar bear subpopulation

```
## FUNCTION DESCRIPTION: Population projection for female polar bears using a theta-logistic model of density dependence

## INPUTS:
## tsteps [scalar] : number of annual timesteps (t = 1,2,...k) for population projection; example tsteps = 35
## N.1 [scalar or vector] : female abundance (N) at t = 1, either point estimate or sampling distribution; example N.1 = 1000 or c( 999, 1001, 882,... )
## se.N1 [scalar] : standard error of female abundance at t = 1, only relevant if point estimate of N.1 was specified; example se.N1 = 100
## start.yr [scalar] : starting year of projections, for indexing only; example start.yr = 2016
## NoverK.start [scalar] : population density at t = 1 expressed as abundance (N) divided by carrying capacity (K); example NoverK.start = 0.7
## prop.f.start [scalar] : proportion of females at t = 1; fixed to prop.f.start = 1
## rmax [ scalar or vector ] : maximum intrinsic growth rate at each timestep, either point estimate or sampling distribution; example rmax = 0.10 or c( 0.11, 0.08, 0.9,... )
## se.rmax [ scalar ]: standard error of estimated maximum intrinsic growth rate, only relevant if point estimate or rmax was specified; example se.rmax = 0.02
## mgmt.interval [scalar ] : number of years elapsed between simulated subpopulation assessments and adjustments to harvest level; example mgmt.interval = 5
## N.rsd [ scalar ] : relative standard deviation in estimates of N from simulated subpopulation assessments; example N.rsd = 0.25
## theta [ scalar ] : shape parameter in discrete version of the theta-logistic equation; fixed to theta = 5.045
## H.type [ character = "fixed.level", "fixed.rate", "state1", "none" ] : type of harvest management approach; example H.type = "state1"
## Hf.mat [ matrix with nrow = nsamples and ncol = tsteps-1 ] : female harvest rate or havest level at each timestep
## Hm.mat [ matrix with nrow = nsamples and ncol = tsteps-1 ] : male harvest rate or havest level at each timestep
## K.proxy [vector with length = k] : proxy for carrying capacity at each timestep; fixed to NULL
## nsamples [ scalar ] : number of samples from the distributions of N and r for which to run stochastic projections
## plot.it [ boolean ] : should projections be plotted; example plot.it = TRUE

## OUTPUT: list containing the following objects
## DD.results [ matrix ] : rows correspond to samples of biological parameters, columns are starting N, rmax, maximum net productivity level (MNPL), r at MNPL, and yield at MNPL
## DD.summary [ matrix ] : summary statistics for columns of DD.results
## pop.results [ matrix ] : rows correspond to timesteps, columns are t, N, K, observed growth rate, female harvest, male harvest, female recruitment, male recruitment, female abundance, male abundance
## pop.summary [ matrix ] : rows correspond to timesteps, new columens (wrt pop.results) are stochastic subpopulation outcomes
## DD.mat [ matrix ] : this object describes the density-dependent relationships; rows are increments of N/K, columns are N/K, N, observed growth rate, yield

## CONTACT INFORMATION:
## Eric V Regehr, PhD
## Polar Science Center - Applied Physics Laboratory
## Box 355640
## University of Washington
## 1013 NE 40th Street
```

```
## Seattle, WA 98105-6698
## Email:  eregehr@uw.edu

## This represents one of several functions, which have variable formatting and organization, that were used for subpopulation projections
## in the following report:

## Regehr, E., M. Dyck, G. Gilbert, S. Iverson, D. Lee, N. Lunn, J. Northrup, A. Penn, M.-C. Richer and G. Szor. 2019.
## Provisional Harvest Risk Assessment for the Southern Hudson Bay Polar Bear Subpopulation. Report to the Southern
## Hudson Bay Polar Bear Subpopulation Advisory Committee, 07 June 2019. Unpublished report. 75 pp.

## DISCLAIMER: The authors provide no guarantee regarding the completeness or functionality of these data and programs,
## and are not responsible for any consequences of their use.

#----
#----
#----
#----

F.theta.proj <- function( tsteps, N.1, se.N1, start.yr, NoverK.start, prop.f.start = 1,
                         rmax, se.rmax, rmax.change = NULL, mgmt.interval = NULL, N.rsd = NULL, theta = 5.045,
                         H.type, Hf.mat, Hm.mat = NULL, Nthr = NULL, Nthr.close = FALSE,
                         K.proxy, nsamples, female.only = TRUE, plot.it = FALSE ) {  #Open over main function


#Load required libraries

#Record functon call
function.call <- match.call()

  #Define range of densities over which to generate objects
  NoverK.t <- seq( from = 0.001, to = 2, by = 0.001 )

  #Standardize proxy for K to equal 1 in the first year of projections
  K.proxy <- K.proxy / K.proxy[[1]]

  #Generate sampling distribution vectors for N and rmax, with expected value in first position
  if( length(rmax) == 1 ) {
  rmax.samplevec <- c(rnorm( n = nsamples , mean = rmax, sd = se.rmax ) )
  rmax.samplevec[[1]] <- rmax }  #the first sample is the specified expected value of the parameter
  if( length(rmax) > 1 ) { rmax.samplevec <- rmax; rmax.samplevec[[1]] <- mean(rmax.samplevec) }
```

```
if( length(N.1) == 1 ) {
N.1.samplevec <- c(rnorm( n = nsamples , mean = N.1, sd = se.N1 ) )
N.1.samplevec[[1]] <- N.1 } #the first sample is the specified expected value of the parameter
if( length(N.1) > 1 ) { N.1.samplevec <- N.1; N.1.samplevec[[1]] <- mean(N.1.samplevec) }



#Initialize arrays to hold results
a1 <- c( "t", "N", "K", "r.obs", "H.f", "H.m", "B.f", "B.m", "N.f", "N.m" )
pop.results <- array( 0, dim = c( tsteps, length(a1), nsamples ) )
dimnames(pop.results) <- list( start.yr:(start.yr+tsteps-1), a1, 1:nsamples )
a1 <- c( "N.1", "rmax", "MNPL", "r.MNPL", "yield.MNPL" )
DD.results <- matrix( NA, nrow = nsamples, ncol = length(a1) )
colnames(DD.results) <- a1

#Create indicator for when to udpate harvest rate under state-dependent management
update.h.ind <- NULL
if( H.type == "state1" ) { update.h.ind <- seq( from = 2, to = tsteps, by = mgmt.interval ) }

#----

#Loop over samples
for( z in 1:nsamples ) {  #Open loop over z over nsamples of the biological parameters

#Select current values of population parameters
N.1 <- N.1.samplevec[[z]]
rmax <- rmax.samplevec[[z]]
if( rmax <= 0 ) { rmax <- 0.0001 }

#Starting sex-specific abundance
N.1.f <- N.1 * prop.f.start
if( N.1.f <= 0 ) { N.1.f <- 1 }
N.1.m <- N.1 * ( 1 - prop.f.start )  #not currently used

#Harvest vector for current sample
Hf <- Hf.mat[ z, ]
ifelse( is.null(Hm.mat), Hm <- rep( 0, length(Hf) ), Hm <- Hm.mat[ z, ] )
```

```
#Vector with time-dependent values of carrying capacity
K <- K.proxy[ z, ] * N.1 / NoverK.start

#Generate density-dependent objects using a theta logistic equation formulated per Morris and Doak (2002) page 102
if( rmax > 0.001 ) {
r.obs <- log( exp( rmax * ( 1 - NoverK.t^theta ) ) ); names(r.obs) <- NoverK.t
N <- K[[1]] * NoverK.t
yield <- N * r.obs
ind1 <- ( which( yield == max(yield) ) )[[1]]
MNPL <- NoverK.t[[ind1]]
yield.MNPL <- yield[[ind1]]
r.MNPL <- r.obs[[ind1]] }

#set all possible growth rates to rmax, if rmax is negative
if( rmax < 0.001 ) {
r.obs <- rep( rmax, length(NoverK.t) )
N <- K[[1]] * NoverK.t
yield <- rep( 1, length(NoverK.t) )
MNPL <- NA
yield.MNPL <- 0
r.MNPL <- rmax }

if( z == 1 ) { DD.mat <- data.frame( NoverK.t, N, r.obs, yield ) }  #save full DD objects for specified parameter values only

#Populate initial values
DD.results[ z, "N.1" ] <- N.1
DD.results[ z, "rmax" ] <- rmax
DD.results[ z, "MNPL" ] <- MNPL
DD.results[ z, "r.MNPL" ] <- r.MNPL
DD.results[ z, "yield.MNPL" ] <- yield.MNPL

#Populate the first row of results matrix
pop.results[ , "t", z ] <- 1:tsteps
pop.results[ 1, "N.f", z ] <- N.1.f
pop.results[ 1, "N.m", z ] <- N.1.m
pop.results[ 1, "N", z ] <- N.1.f + N.1.m
pop.results[ , "K", z ] <- K

#----
```

```
#Loop over years
for( i in 2:(tsteps) ) {  #Open loop over i tsteps

  #Extract values at current timestep
  N.t <- pop.results[ i-1, "N", z ]
  K.t <- pop.results[ i-1, "K", z ]
  N.f.t <- pop.results[ i-1, "N.f", z ]
  N.m.t <- pop.results[ i-1, "N.m", z ]

  #Calculate harvest level to be implemented prior to population growth
  if( H.type == "fixed.level" ) {
     Hf.t <- Hf[[ i-1 ]]
     Hm.t <- Hm[[ i-1 ]] }

  if( H.type == "fixed.rate" ) {
     Hf.t <- Hf[[ i-1 ]] * N.t
     Hm.t <- Hm[[ i-1 ]] * N.t }

  if( H.type == "state1" ) {  #open over state1 for baseline state-dependent management

    #Indicator for whether it is an occasion on which to perform a simulated population assessment and update harvest level
    #under a state-dependent mgmt approach
    h.estimate.ind <- ( i %in% update.h.ind )

       #At the start of projections (i = 2) harvest is based on the expected values of parameter estimates from the case study, rather than
       #on the current sample of parameter estimates
       if( ( h.estimate.ind ) & ( i == 2 ) ) {  #Open over if i = 2

       #Calculate the recommended harvest level based on the specified harvest rate and starting abundance
       N.est.h <- N.1.samplevec[[1]]
       Hf.t <- N.est.h * Hf[[i-1]]
       Hm.t <- N.est.h * Hm[[i-1]]
       }  #Close over if i = 2


    #For occasions i > 2 on which the harvest is updated under a state-dependent approach, calculate harvest level from
    #estimated value of N and the specified harvest rate
    if( ( h.estimate.ind ) & ( i > 2 ) ) { #open over if h.estimate.ind

       a1 <- mean( pop.results[ (i-3):(i-1), "N", z ] )  #mean total abundance for the 3 preceding timesteps
```

```
      N.est.h <- rnorm( n = 1, mean = a1, sd = N.rsd * a1 )  #this assumes that the 50th percentile of estimated N is used
      Hf.t <- N.est.h * Hf[[i-1]]
      Hm.t <- N.est.h * Hm[[i-1]]

      #If there is a harvest closure threshold, evaluate and implement
      if( Nthr.close == TRUE ) { if( N.est.h < Nthr) { Hf.t <- 0; Hm.t <- 0 } }
      }  #close over h.estimate.ind
    }  #close over state1


  #Naming convention
  Hf.t.mod <- Hf.t
  Hm.t.mod <- Hm.t

  #Apply excess male harvest to females
  if( is.null(Hm.mat) == FALSE ) { if( Hm.t > N.m.t ) {  Hm.t.mod <- max( c( N.m.t, 0 ) ); Hf.t.mod <- Hf.t + ( Hm.t - max( c( N.m.t, 0 ) ) ) } }  #not currently
used

  #Don't allow harvest levels to be negative
  Hf.t.mod <- ifelse( Hf.t.mod < 0, 0, Hf.t.mod )
  Hm.t.mod <- ifelse( Hm.t.mod < 0, 0, Hm.t.mod )

  #Population size for females and males after harvest
  N.f.t <- N.f.t - Hf.t.mod
  N.m.t <- N.m.t - Hm.t.mod  #not currently used


  #End projection if population size is below quasi-extinction threshold
  if( ( N.f.t < ( 0.15 * N.1 ) ) | ( N.f.t < 0 ) ) { break }


  #Retrieve current growth rate as a function of post-harvest population density
  ind1 <-  which( abs( ( ( N.f.t + N.m.t ) / K.t ) - NoverK.t ) == min( abs( ( ( N.f.t + N.m.t ) / K.t ) - NoverK.t ) ) )
  r.obs.t <- r.obs[[ ind1 ]]

  #If rmax changes as a function of the ice proxy, use the updated value
  if( is.null( rmax.change ) == FALSE )
  #{ a1 <- rmax * K.proxy[ z, i - 1 ]
  #  r.obs.t <- log( exp( a1* ( 1 - ( ( N.f.t + N.m.t ) / K.t )^theta ) ) ) }
  { a1 <- rmax + i * rmax * rmax.change
```

```
    a1 <- ifelse( a1 <= 0, 0.001, a1 )
    r.obs.t <- log( exp( a1* ( 1 - ( ( N.f.t + N.m.t ) / K.t )^theta ) ) ) }

  #Calculate the change in population size assuming equal sex ratio at birth and no mechanisms of reproduction
  B.f <- ( ( N.f.t + N.m.t ) * r.obs.t )
  if( female.only == TRUE ) { B.m <- 0 }  #no male recruitment if the run is female only

  #Calculate post-harvest and growth population size
  N.f.cur <- N.f.t + B.f
  N.m.cur <- N.m.t + B.m
  N.cur <- N.f.cur + N.m.cur

  #End projection if population size is below quasi-extinction threshold
  if( ( N.cur < ( 0.15 * N.1 ) ) | ( N.f.cur < 0 ) ) { break }


  #Store results
  pop.results[ i, "N", z ] <- N.cur
  pop.results[ i, "N.f", z ] <- N.f.cur
  pop.results[ i, "N.m", z ] <- N.m.cur
  pop.results[ i-1, "r.obs", z ] <- r.obs.t
  pop.results[ i-1, "B.f", z ] <- B.f
  pop.results[ i-1, "B.m", z ] <- B.m
  pop.results[ i-1, "H.f", z ] <- Hf.t.mod
  pop.results[ i-1, "H.m", z ] <- Hm.t.mod

  } #Close loop over tsteps
  } #Close loop over nsamples

#----

 #Summarize resuts across samples, if multiple samples of the biological parameters are considerd within F.theta.proj, rather than looping over the function
 DD.summary <- NULL
 pop.summary <- NULL

 if( nsamples > 1 ) {  #Open if over nsamples

 #Density-dependent results
 temp2 <- t( apply( DD.results, 2, function(x) { xout <- c( mean( x, na.rm = TRUE ), median( x, na.rm = TRUE ),
                                        estimate_mode(x), sd( x, na.rm = TRUE ) ); xout } ) )
```

```
temp2 <- cbind( DD.results[ 1, ], temp2 )
temp2 <- round( temp2, digits = 3 )
colnames(temp2) <- c( "actual", "mean", "median", "mode", "sd" )
DD.summary <- temp2

#Remove final, incomplete row of population results
pop.results <- pop.results[ -1 * dim(pop.results)[[1]], , ]

#Calculate mean value across third dimension (i.e. pages)
temp1 <- apply( pop.results, 1:2, mean, na.rm = TRUE )

#Stochastic probabilities of extirpation and male depletion
a1 <- pop.results[ , "N", ]
prob.ext <- apply( a1, 1, function(x) { sum( x == 0 )/ length(x) } )
a1 <- pop.results[ , "N.m", ]
a2 <- matrix( pop.results[ 1, "N", ], nrow = nrow(a1), ncol = ncol(a1), byrow = TRUE )
a3 <- a1 < ( 0.15 * a2 * .5 )
prob.male.dep <- apply( a3, 1, function(x) { sum(x)/ length(x) } )  #not currently used

#Mean proportion female for surviving populations
a1 <- pop.results[ , "N.f", ] / pop.results[ , "N", ]
a1[ is.infinite(a1) ] <- NA
prop.f <- apply( a1, 1, mean, na.rm = TRUE )

#Probability of N > MNPL
a1 <- pop.results[ , "N", ]
a2 <- pop.results[ , "K", ]
a3 <- a1 >= ( 0.7 * a2 )
P.MNPL <- apply( a3, 1, function(x) { sum( x == TRUE )/ length(x) } )

#Probability of N > 0.9N1
a1 <- pop.results[ , "N", ]
a2 <- matrix( pop.results[ 1, "N", ], nrow = nrow(a1), ncol = ncol(a1), byrow = TRUE )
a3 <- a1 >= ( 0.9 * a2 )
P.9N1 <- apply( a3, 1, function(x) { sum( x == TRUE )/ length(x) } )

#Probablity of N > threshold subpopulation size
P.Nthr <- rep( NA, length(P.9N1) )
if( is.null(Nthr) == FALSE ) {
a1 <- pop.results[ , "N", ]
```

```
  a2 <- matrix( pop.results[ 1, "N", ], nrow = nrow(a1), ncol = ncol(a1), byrow = TRUE )
  a3 <- a1 >= Nthr
  P.Nthr <- apply( a3, 1, function(x) { sum( x == TRUE )/ length(x) } ) }

  #Probability that harvest was closed due to threshold rule
  P.Hclose <-  rep( NA, length(P.9N1) )
  if( Nthr.close == TRUE ) {
  a1 <- pop.results[ , "H.f", ]
  P.Hclose <- apply( a1, 1, function(x) { sum( x == 0 )/ length(x) } ) }


  #Consolidate summary data
  pop.summary <- as.data.frame( cbind( temp1[ , c( "N", "K", "H.f", "H.m" ) ], prob.ext, prop.f, prob.male.dep, P.MNPL, P.9N1, P.Nthr, P.Hclose ) )
  }  #Close if over nsamples

  #----

#Consolidate full results list
results.list <- list( DD.results = DD.results, DD.summary = DD.summary, pop.results = pop.results,
                      pop.summary = pop.summary, DD.mat = DD.mat )


#Plot a sample of projections
if( plot.it == TRUE ) {

results <- pop.results
if( nsamples == 1 ) { a1 <- ( results[ , "K", , drop = FALSE ] ) }
if( nsamples > 1 ) { a1 <- ( results[ , "K", ] ) }

temp.K <- t( apply( a1, 1, function(x) { xout <- c( mean(x), quantile( x, probs = c( 0.025, 0.975 ) ) ); xout } ) )
colnames(temp.K)[[1]] <- "mean"

if( nsamples == 1 ) { temp.N <- ( results[ , "N", , drop = FALSE ] ) }
if( nsamples > 1 ) { temp.N <- ( results[ , "N", ] ) }

x <- as.numeric( rownames(temp.N) )
par( mar = c( 7.6, 7.6, 4.6, 2.1 ) )
matplot( x = x, y = temp.N, ylim = c( 0, ( 1.5 * max( temp.K[ , "mean" ] ) ) ),
       xlab = "", ylab = "", cex.lab = 1.8, cex.axis = 2, cex.main = 2.25,
       type = "n", main = "" )
```

```
matplot( x = x, y = temp.N[ , 1:(ifelse( nsamples >= 100, 100, nsamples)) ], type = "l", lty = 1, lwd = 0.25, add = TRUE, col = blackt1 )
lines( x = x, y = apply( temp.N, 1, mean ), type = "l", lwd = 6, lty = 1, col = "black" )  #mean

polygon( c( rev(x), x ), c( rev( temp.K[ , "2.5%" ] ), temp.K[ , "97.5%" ] ), col = grayt1, border = NA)
lines(x = x, y = temp.K[ , "mean" ], lty = 3, lwd = 8, col = grayt2 )  #median

mtext( text = "Year", side = 1, cex = 2, line = 4.5 )
mtext( text = "Female abundance", side = 2, cex = 2, line = 4.5 )              }

#Return results object
return( results.list )

}  #Close over main function



#----
#----
#----
#----


#Utility function to estimate mode of a vector
estimate_mode <- function( x, na.rm = TRUE ) {
  if( na.rm == TRUE ) { x <- x[ is.na(x) == FALSE ] }
  if( na.rm == FALSE ) { if( TRUE %in% is.na(x) ) { stop("\nThere are NA values in the data\n") } }
  d <- density(x)
  d$x[which.max(d$y)]
}


#----
```